ACS Chemical Neuroscience

Article

Inhibition of serine palmitoyltransferase by a small organic molecule promotes neuronal survival after astrocyte amyloid beta 1-42 injury

Teresa De Vita, Clara Albani, Natalia Realini, Marco Migliore, Abdul Basit, Giuliana Ottonello, and Andrea Cavalli

ACS Chem. Neurosci., **Just Accepted Manuscript** • DOI: 10.1021/acschemneuro.8b00556 • Publication Date (Web): 27 Nov 2018

Inhibition of serine palmitoyltransferase by a small organic molecule promotes neuronal survival after astrocyte amyloid beta 1-42 injury

Teresa De Vita,[†] Clara Albani,[‡] Natalia Realini,[∫] Marco Migliore,[‡] Abdul Basit,[Δ] Giuliana Ottonello,[Δ] and Andrea Cavalli*[, †, §]

[†]Computational and Chemical Biology, Istituto Italiano di Tecnologia, Via Morego 30, 16163 Genova, Italy.

[‡]Drug Discovery and Development, Istituto Italiano di Tecnologia, Via Morego 30, 16163 Genova, Italy.

[∫]D3 Validation, Istituto Italiano di Tecnologia, Via Morego 30, 16163 Genova, Italy.

[Δ]Analytical Chemistry Facility, Istituto Italiano di Tecnologia, Via Morego 30, 16163 Genova, Italy.

[§]Dipartimento di Farmacia e Biotecnologie, Università di Bologna, Via Belmeloro 6, 40126 Bologna, Italy.

Keywords: Alzheimer's disease, ceramides, serine palmitoyltransferase, astrocytes, neurons, neuroinflammation, neuroprotection.

Graphical Abstract

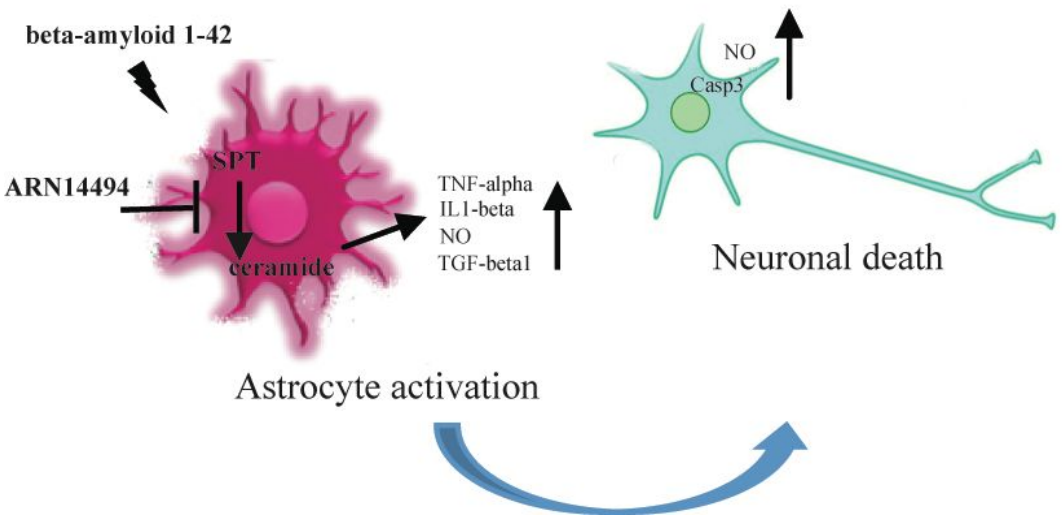

ABSTRACT: Alzheimer's disease (AD) is a slow-progressing disease of the brain characterized by symptoms such as impairment of memory and other cognitive functions. AD is associated with an inflammatory process that involves astrocytes and microglial cells, among other components. Astrocytes are the most abundant type of glial cells in the central nervous system (CNS). They are involved in inducing neuroinflammation. The present study uses astrocyte-neuron co-cultures to investigate how ARN14494, a serine palmitoyltransferase (SPT) inhibitor, affects the CNS in terms of anti-inflammation and neuroprotection. SPT is the first rate-limiting enzyme in the de novo ceramide synthesis pathway. Consistent evidence suggests that ceramide is increased in AD brain patients. After β-amyloid 1-42 injury in an in vitro model of AD, ARN14494 inhibits SPT activity and the synthesis of long-chain ceramides and dihydroceramides that are involved in AD progression. In mouse primary cortical astrocytes, ARN14494 prevents the synthesis of pro-inflammatory cytokines TNFα and IL1β, growth factor TGFβ1, and oxidative stress–related enzymes iNOS and COX2. ARN14494 also exerts neuroprotective properties in primary cortical neurons. ARN14494 decreases neuronal death and caspase-3 activation in neurons, when the neuroinflammation is attenuated in astrocytes. These findings suggest that ARN14494 protects neurons from β-amyloid 1-42-induced neurotoxicity through a variety of mechanisms, including anti-oxidation, anti-apoptosis, and anti-inflammation. SPT inhibition could therefore be a safe therapeutic strategy for ameliorating the pathology of Alzheimer's disease.

INTRODUCTION

The symptoms of Alzheimer's disease (AD) include a progressive loss of memory, neuronal death, inflammation, and a debilitation of intellectual capacity.[1-3] The exact etiopathogenesis of AD is still unclear. According to the amyloid cascade hypothesis, amyloid plaques formed by aggregates of amyloid β (Aβ) peptide generated by the proteolytic cleavages of APP are central to AD pathology. According to the tau hyperphosphorylation hypothesis, the excessive or abnormal phosphorylation of tau is central to AD pathology.[4,5] There are multiple etiological and pathogenetic hypotheses

concerning AD pathogenesis, including oxidative stress[6,7], cholesterol[8], metallobiology[9], dysregulation of neurotransmitters[10-13] and insulin.[14] Although the precise mechanisms are not fully understood, inflammation plays a central role in AD development.[15,16] Aβ promotes an inflammatory response mediated by microglia and astrocytes, stimulating activation. Glial activation involves morphological changes, astrogliosis, including an increase in the number, size, and motility of astrocytes and a change in the expression of many proteins. Astrocyte activation can produce nitric oxide (NO) and other pro-inflammatory mediators, which amplify the inflammatory response.[17-19] Reactive astrocytes also synthesize cytokines, including interleukin-1β (IL-1β), tumor necrosis factor-α (TNF-α), and transforming growth factor β (TGF-β), which contribute to brain inflammation and neuronal injury.[20-24] There is consistent support for a link between ceramides and AD. Several studies have demonstrated the involvement of saturated fatty acids in neuroinflammation mediated by glial cells. Ceramides, a class of sphingolipids, are increased in AD patients[25-27] and may contribute to AD pathogenesis. Serine palmitoyltransferase (SPT) catalyzes the first step in sphingolipid biosynthesis. In AD, it regulates ceramide levels through elevated serine palmitoyltransferase long chain 1 (SPTLC1) and serine palmitoyltransferase long chain 2 (SPTLC2) levels.[28] Activation of SPT increases ceramide levels, whereas inhibition decreases ceramide levels, both in vitro and in vivo.[29,30] In addition, inhibiting the de novo ceramide synthesis decreases Aβ production, while exogenous ceramides increase Aβ production.[31] SPT is therefore considered a novel target for AD treatment. SPT condenses the palmitic acid of the precursor palmitoyl-coenzyme A with serine to produce ketosphinganine, the precursor characteristic of all sphingolipids[32]. This is the first step in the de novo ceramide synthesis pathway.[33,34] SPT comprises two different subunits, LCB1 and LCB2. Two additional small subunits confer full enzymatic activity to the protein.[35] Malfunctioning of SPT correlates with many pathological conditions including emphysema[36], cardiovascular disease[37], and metabolic disorders.[38] Activation of astrocytes by palmitic acid is mediated by SPT, and activated astrocytes increase β-secretase (BACE1) levels in neurons.[39] In addition, subcutaneous administration of L-cycloserine, one of the few available SPT inhibitors,

downregulates levels of both Aβ and phosphorylated tau in murine cortex,[40] pointing to SPT inhibition as a possible therapeutic strategy for AD. There are currently very few known SPT inhibitors. In 2008, Pfizer filed a patent for a series of novel SPT inhibitors, mainly for cardiovascular diseases and metabolic disorders. (Patent: WO2008/084300) Here, using a novel synthetic strategy, we synthesized and characterized the most promising compound, ARN14494. This compound was characterized in neuronal cells to determine its ability to reduce ceramide levels and SPT activity in vitro. In addition, we used a β-amyloid-induced inflammatory model in cortical astrocyte-neuron co-cultures to investigate ARN14494's effects. ARN14494 displayed anti-inflammatory and neuroprotective effects in the context of Aβ 1-42 injury.

RESULTS AND DISCUSSION

In the present study, we characterized a new SPT inhibitor, ARN14494 as a new tool for AD treatment. ARN14494 was obtained by a novel synthetic strategy reported in Table 1. Compound **7** was prepared according to a modified procedure reported by Pfizer (WO2008/084300). In brief, commercial acid **1** was converted to the corresponding acyl chloride and then reacted with amide **2** in almost quantitative yield. Aromatic nucleophilic substitution at the fluorine center with ditertbutylmalonate gave in good yield compound **3**. Catalytic hydrogenation of **3** in the presence of 10% palladium on carbon afforded quantitatively the amine **4** which was reacted with BOC-piperidone under reductive amination conditions to obtain the N-alkylated piperidine **5**. Sequential deprotection of the BOC, hydrolysis of both tertbutyl esters, decarboxylation and ring closure gave in excellent yield the lactam **6**. Nucleophilc substitution of **6** with the corresponding chloroacetamide (WO2008/084300) afforded the target molecule **7** in good yield.

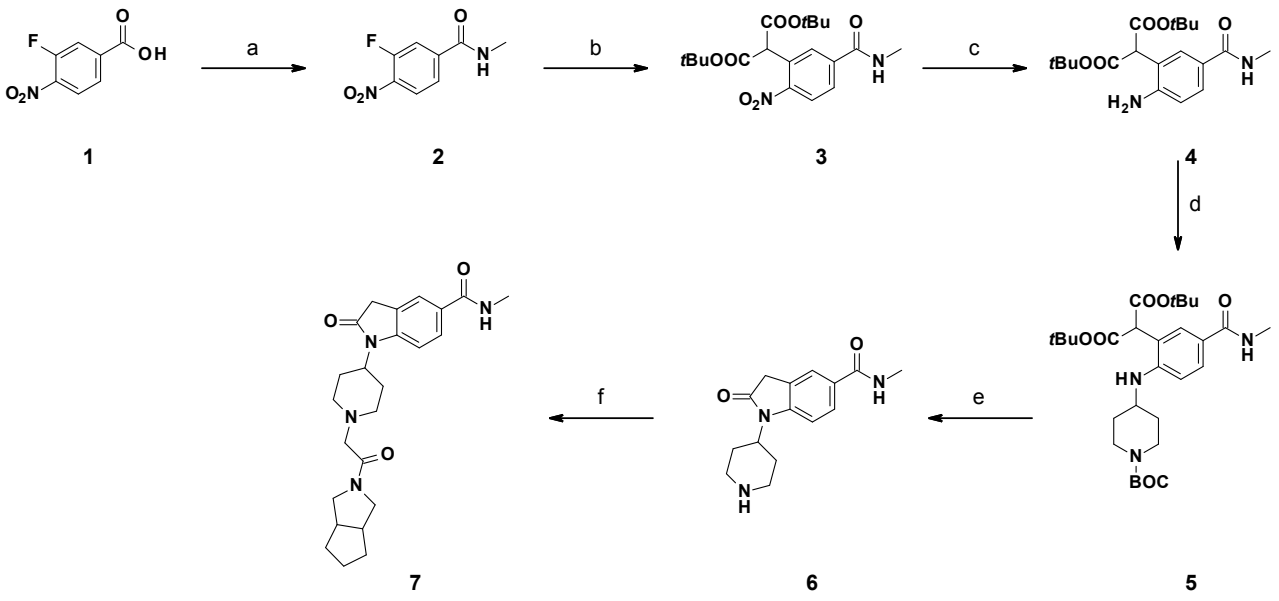

Table 1. Synthesis of compound ARN14494. **a)** oxalyl chloride; $MeHN_2 \cdot HCl$, TEA, H_2O, 0 °C, 94%; **b)** ditButylmalonate, NaH, DFM, 64%; **c)** Pd/C, $HCOONH_4$, MeOH, 100%; **d)** *N*-BOC-piperidone, AcOH, $NaBH(OAc)_3$, DCE, 60%; **e)** TosOH, Tol/H_2O, 100 °C, 87%; **f)** R-$COCH_2Cl$, K_2CO_3, ACN/H_2O, 68%.

ARN14494 was tested in vitro on microsomal preparations of HEK293. The compound showed SPT inhibition activity with a mean effective concentration (IC50) of 27.3 ± 3.06 nM. This compound was originally reported by Pfizer for the treatment of cardiovascular diseases and metabolic disorders (WO2008/084300) and was here initially characterized in two neuronal cell lines: mouse neuroblastoma Neuro-2a and human astrocytoma CCF-STTG1 cells. Cultures of Neuro-2a and CCF-STTG1 cells treated with ARN14494 for 24 h displayed a concentration-dependent reduction in SPT activity (Figure 1A, B). The ability of the compound to inhibit SPT activity on cell cultures is lower when compare to the inhibition activity demonstrated on HEK293 microsomal preparations and is respectively: N2a IC50= 9.5 ± 6.36 μM and CCF-STTG1 IC50= 10 ± 8.48 μM. This inhibition was accompanied by a reduction of the de novo synthesis of total ceramide and dihydroceramide levels in Neuro-2a cells (Figure 1C, E) and CCF-STTG1 cells (Figure 1D, F), which were identified and quantified by liquid chromatography/mass spectrometry (LC/MS).

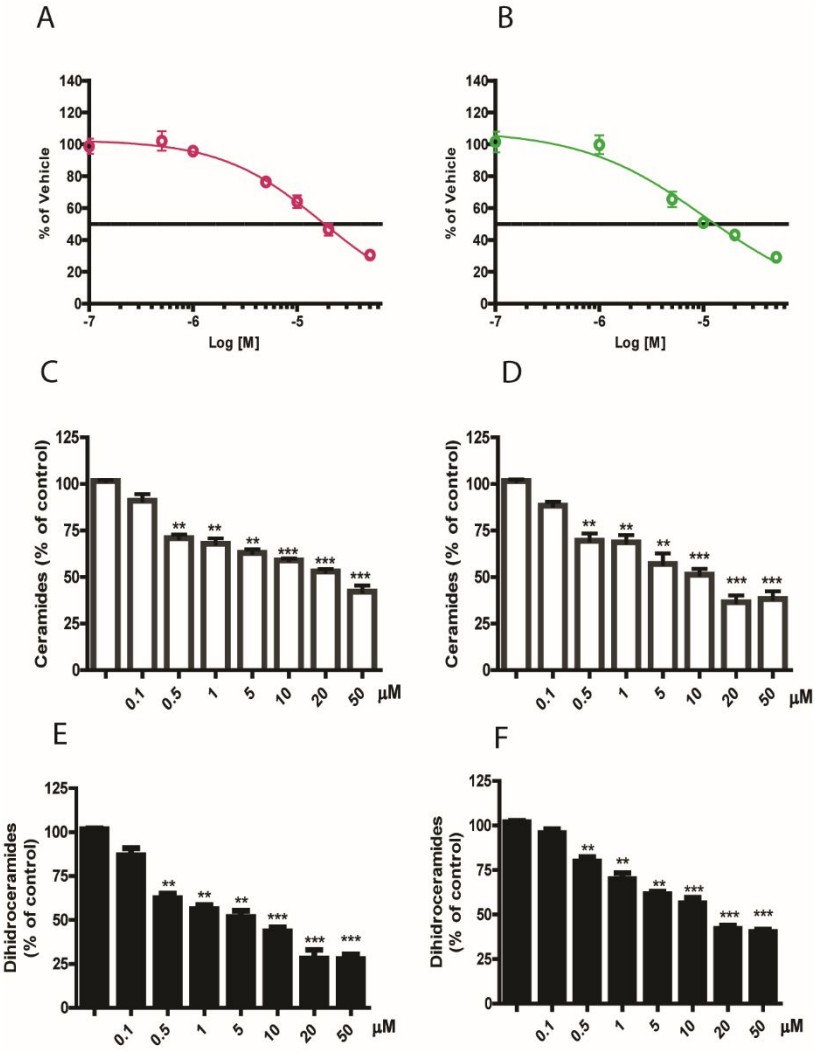

Figure 1. ARN14494 is a potent SPT inhibitor, and it decreases ceramide and dihydroceramide levels in mouse Neuro-2a and human CCFSTTG1 cells. Effects of ARN14494 (n=3) on SPT activity in mouse N2a (Fig. 1A) and human CCFSTTG1 (Fig. 1B) cells. Effects of ARN14494 on ceramide and dihydroceramide levels in Neuro-2a (Fig. 1 C-E) and CCFSTTG1 (Fig. 1 D-F) cells. Data represent mean ± SEM of three independent experiments performed in triplicate. **p<0.01, ***p<0.001 vs CTRL. One-way ANOVA followed by Newman-Keuls test.

Cultured astrocytes and neurons were used to demonstrate how ARN14494 could have anti-inflammatory and neuroprotective properties. We investigated the effects of ARN14494, using a β-amyloid-induced inflammatory model in cortical astrocyte-neuron co-cultures. Primary mouse astrocytes were treated with different concentrations of β-amyloid 1-42 (Aβ1-42) for 24 h. The activity levels of SPT increased significantly in astrocytes upon treatment with Aβ1-42 10 µM (Figure 2A). For subsequent experiments treating astrocytes with ARN14494, we selected the dose of Aβ1-

42 10 μM. The coadministration with a dose-dependent amount of ARN14494 (1-5-10 μM) caused a concentration-dependent reduction in SPT activity (Figure 2B).

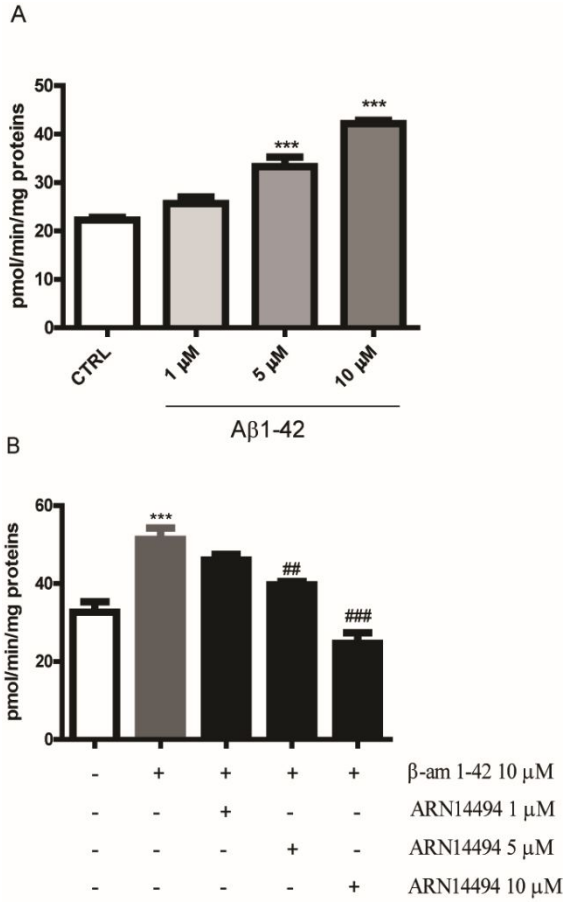

Figure 2. ARN14494 inhibits SPT activity in mouse primary astrocytes. Effect of an increase dose of Aβ1-42 on SPT activity in mouse primary astrocytes (Fig. 2A). Effect of an increase of ARN14494 on SPT activity in mouse primary astrocytes (Fig 2B). Data represent mean ± SEM of three independent experiments. ***p<0.001 vs CTRL, ##p<0.01, ###p<0.001 vs Aβ1-42. One-way ANOVA followed by Newman-Keuls test.

Ceramides can be formed by de novo synthesis through the action of SPT. Ceramides with various chain lengths can influence different cellular processes and are critical in several diseases. In AD patients, accumulation of C:18 and C:24 ceramides is associated with disease progression.[25] This led us to investigate ceramides of different lengths. Astrocytes treated with an increased dose of Aβ1-42 (1-5-10 μM) showed increased ceramide levels of (d16:0) and its precursor dihydroceramide (d16:0). We observed similar results with other species of sphingolipids: ceramide (d18:0), (d24:0), (d24:1),

and dihydroceramides (d18:0), (d24:0), (d24:1). The major effect was observed using Aβ1-42 10 μM (Supplementary Figure S1A-B). We next treated astrocytes with Aβ1-42 10 μM for 24 h. The increase of ceramides (d16:0), (d18:0), (d24:0), (d24:1), and dihydroceramides (d16:0), (d18:0), (d24:0), (d24:1) observed after Aβ1-42 administration was completely blocked by incubating astrocytes with 10 μM ARN14494 (Figure 3A-B). These results agree with inhibition of SPT by ARN1449.

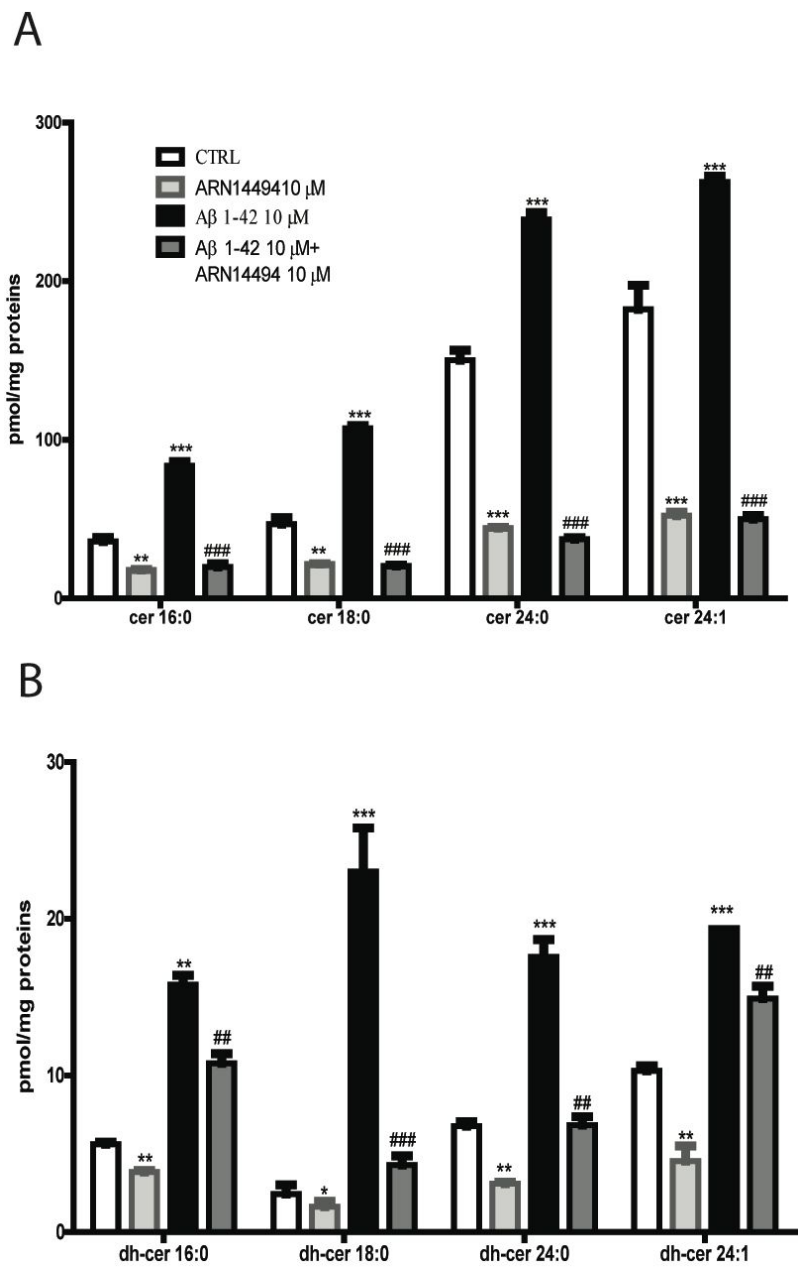

Figure 3. ARN14494 decreases ceramide and dihydroceramide levels in primary cortical astrocytes treated with Aβ1-42. Effects of ARN14494 at 24h of incubation on different ceramide (A) and dihydroceramide (B) levels on mouse primary astrocytes treated with Aβ1-42 10μM. Data represent mean ± SEM of three independent experiments performed in triplicate. *p<0.05, **p<0.01, ***p<0.001 vs ctrl, ##p<0.01, ###p<0.001 vs Aβ1-42 10μM. Two-way ANOVA followed by Bonferroni's test.

In addition to the production of cytokines TNFα and IL1β, the amyloid β plaques also produce growth factor such as TGFβ1 in glial cells and neurons.[41,42] TGFβ1 exerts mostly anti-apoptotic and anti-inflammatory functions, and is involved in several neurodegenerative diseases including AD. Increased levels of TGFβ1 were found in AD brain.[43] Here, we demonstrated that ARN14494 can decrease mRNA levels and protein release of TGFβ1 in astrocytes treated with Aβ1-42 (Figure 4). We examined the possible effects of ARN14494 in suppressing the release of TNF-α, IL-1β, and TGFβ in mouse primary astrocytes. We measured the mRNA levels of TNF-α, IL-1β, and TGFβ1 at various time points (3 h, 6 h, 12 h, 24 h) and found them to be upregulated in the astrocytes treated with Aβ1-42 10μM (Figure 4A,B,C). TNF-α and IL-1β mRNA levels increased significantly after 3 h, with a maximum rate increase between 3 h and 6 h. The highest level of TGFβ1 mRNA was reached after 24 h. When astrocytes were exposed to Aβ1-42 10μM, the accumulation of TNF-α, IL-1β, and TGFβ1 was observed at 24 h. To investigate the anti-inflammatory properties of ARN14494, we treated astrocytes with 10μM ARN14494 and found significantly decreased mRNA levels of TNF-α, IL-1β, and TGFβ1 (Figure 4A-B-C). 10 μM ARN14494 inhibited the expression of TNF-α, IL-1β, and TGFβ1 in Aβ-astrocyte cells (Figure 4D).

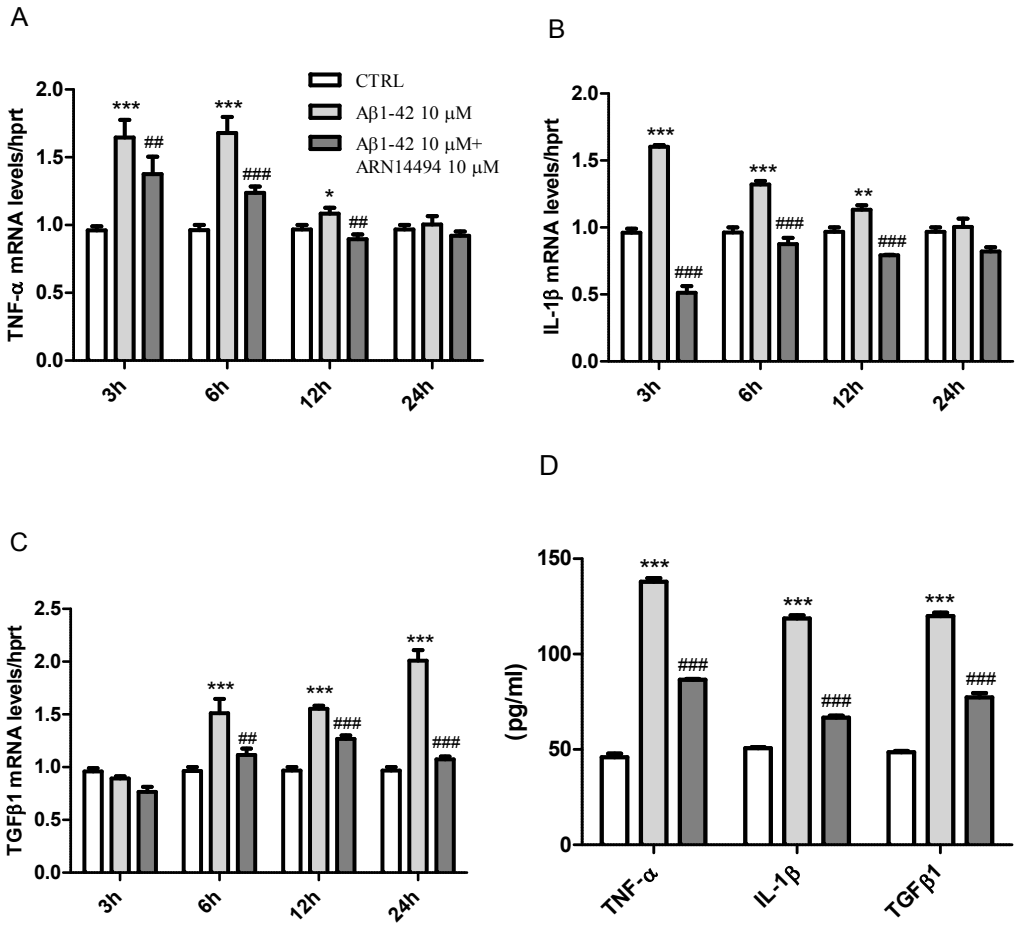

Figure 4. Effect of ARN14494 on Aβ1-42-induced expression of TNF-α, IL1 β, and TGF-1β mRNA and production of TNF-α, IL1 β, and TGF-1β. Primary astrocytes were pretreated with 10 μM of ARN14494 for 24 h. Intact cells were treated with 10 μM of Aβ1-42, then TNF-α (A), IL1 β (B), and TGF-1β (C) mRNA expression was measured 3-6-12-24 h later in cell lysates. Protein production was measured 24 h later in cell medium (D). Data represent mean ± SEM of three independent experiments. *p<0.05, **p<0.01, ***p<0.001 vs CTRL, #p<0.05, ##p<0.0, ###p<0.001 vs Aβ1-42. One-way ANOVA followed by Newman-Keuls test.

Astrocyte activation can produce NO, a diffusible gas involved in the pathogenesis of several neurodegenerative disorders. At higher concentrations, NO is neurotoxic. NO can induce neuronal damage by disrupting the neuronal mitochondrial electron transport chain.[44] Increased levels of iNOS mRNA and enzymatic activity have been demonstrated in animal models of cerebral ischemia.[45] Among the different pro-inflammatory parameters that we evaluated in astrocyte cultures in response

to Aβ, we also observed a dose-dependent reduction of NO production in the culture media (Supplementary Figure S2). Our results suggest that ARN14494 treatment significantly prevented an increase in NO levels as induced by Aβ1-42. The inhibitory effect of ARN14494 on this neurotoxic molecule is likely related to the regulation of the expression of iNOS, responsible for NO synthesis. In agreement, iNOS mRNA and protein expression were upregulated in Aβ1-42-activated astrocytes after 24 h. Pre-treatment with ARN14494 10 μM reduced iNOS expression (Figure 5 A,B). Moreover, COX-2 is frequently observed in a wide range of inflammatory disease. COX-2 induction and subsequent production of prostaglandins by activated microglia and astrocytes is known to be one of the major contributors to neuroinflammation. According to our study, Aβ1-42 increased COX-2 expression at the mRNA and protein levels (Figure 5C-D), most probably by inhibition of NF-kB. Moreover, COX2 expression was markedly inhibited by ARN14494 10 μM. These results suggest that ARN14494 suppresses the expression of neuroinflammatory molecules in Aβ-stimulated astrocytes

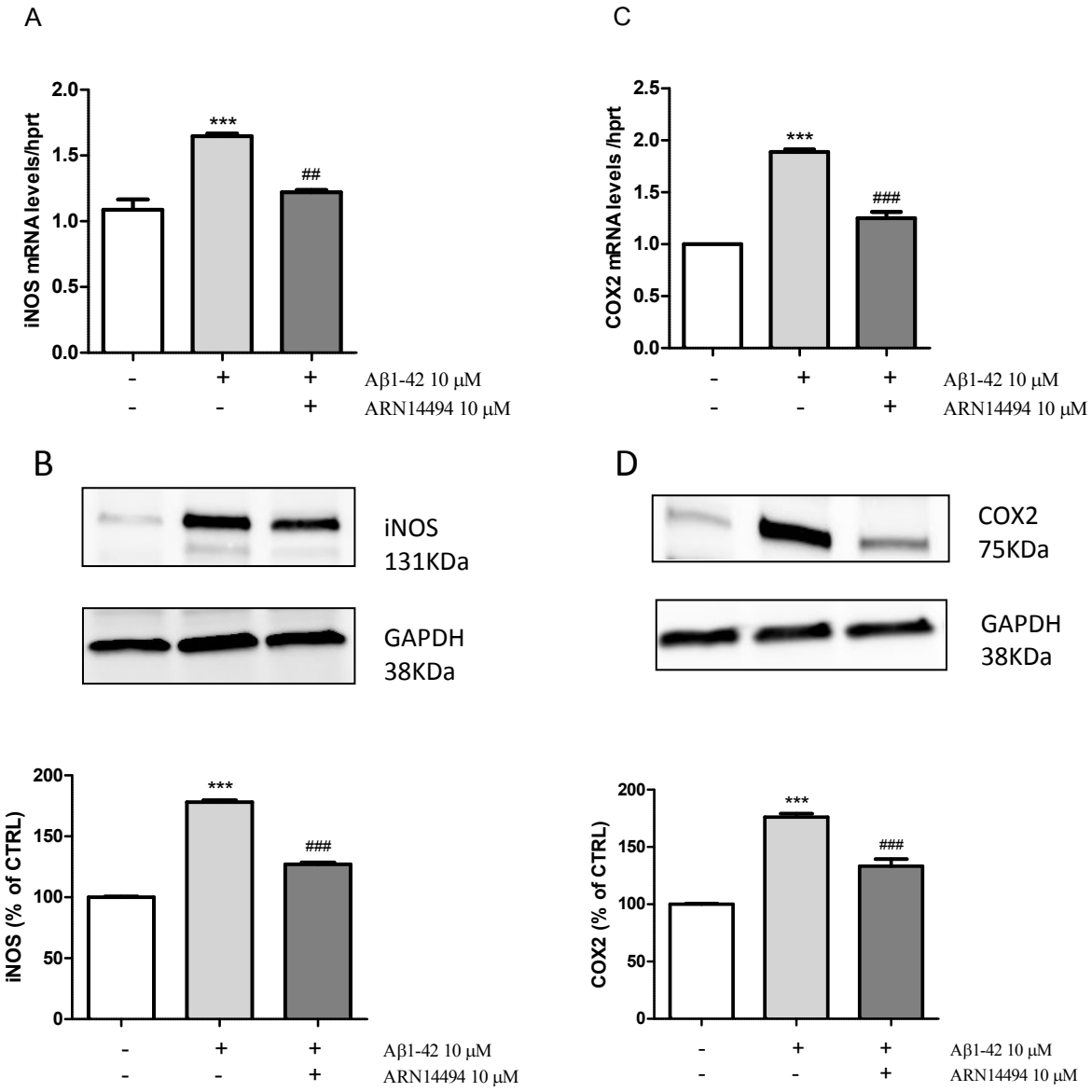

Figure 5. Effect of ARN14494 on Aβ1-42-induced iNOS, COX2 mRNA expression and iNOS, COX2 protein expression. Primary astrocytes were pretreated with 10 μM of ARN14494 for 24 h. Intact cells were treated with 10 μM of Aβ1-42, then iNOS (A) and COX2 (C) mRNA expression was measured 6 h later in cell lysates. The protein expression of iNOS (B) and COX2 (D) was measured by Western blot 24 h later, and data normalized by GAPDH. Data represent mean ± SEM of three independent experiments. **p<0.01, ***p<0.001 vs CTRL, ##p<0.01 vs Aβ1-42. One-way ANOVA followed by Newman-Keuls test

Aβ1-42 induces morphological changes in astrocytes, but does not cause increased astrocyte cell death.[46] The increased release of inflammatory mediators from astrocytes is associated with neuronal toxicity. Using a β-amyloid-induced inflammatory model in cortical astrocyte-neuron co-cultures, we demonstrated the neuroprotective effects of ARN14494. Astrocytes were treated with ARN14494 10 μM and Aβ1-42 10 μM. The conditioned media was subsequently used to treat the primary neurons for 48 h. We observed a decrease of cell viability, then neuronal death with Aβ1-42 10 μM. Pretreatment of astrocytes with ARN14494 10 μM significantly reduced neuronal death in this model (Figure 6A). These results show that components released in the conditioned media of astrocytes mediate neuronal death, and that ARN14494 is able to counteract this process.

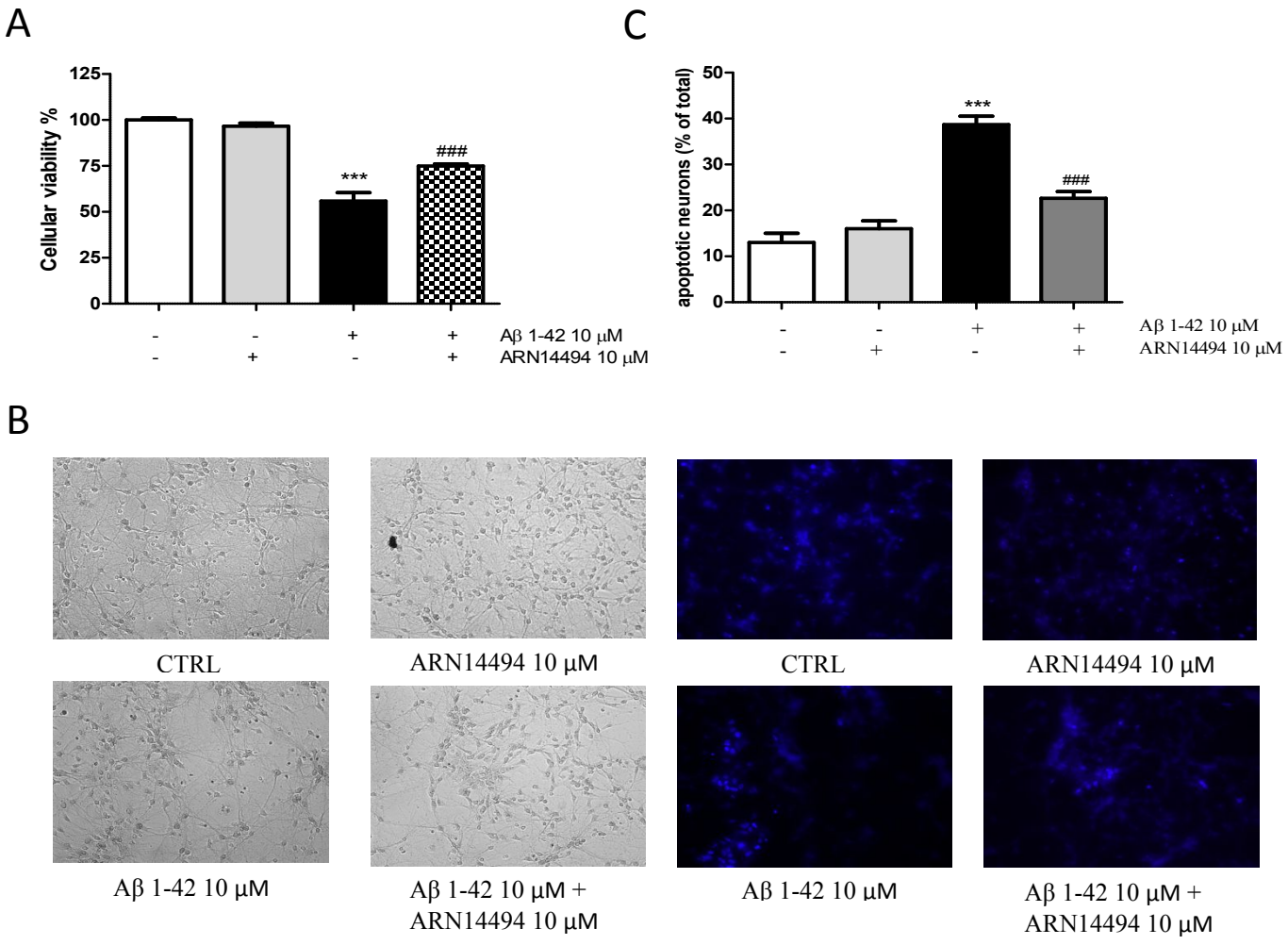

Figure 6. Factors secreted from astrocytes mediate β-amyloid-induced neurotoxicity. Primary cortical neurons were treated for 48 h with conditioned medium from mouse primary astrocytes treated with 10 μM Aβ1-42 and/or 10 μM

ARN14494. Values are ATP release from neurons into medium, expressed as percentage of CTRL (6A). ARN14494 inhibits Aβ1-42-induced neuron apoptosis. (B) The morphological features of apoptosis were monitored by fluorescence microscopy after staining with Hoechst 33342. Neurons that exhibited reduced nuclear size, chromatin condensation, intense fluorescence, and nuclear fragmentation were considered apoptotic. Pretreatment with ARN14494 10 μM for 24 h decreased the number of apoptotic neurons during Aβ1-42 injury. (C) Quantitative analysis of apoptotic neurons. Data represent mean ± SEM of three independent experiments. ***p<0.001 vs CTRL, ###p<0.001 vs Aβ1-42. One-way ANOVA followed by Newman-Keuls test.

Next, we measured neuronal damage. Neuronal toxicity was analyzed by staining with Hoechst 33342. Aβ1-42 10 μM increased the number of apoptotic neurons as compared to controls. Pretreatment with ARN14494 10 μM protected neurons from β-amyloid induced apoptosis (Figure 6B). Quantification of apoptotic neurons is shown in Figure 6C. The finding that astrocytes induce neuronal toxicity led us to investigate caspase-3, an apoptotic marker. Inflammatory mediators are secreted in response to Aβ[46] and active forms of caspase-3 are found in AD brain[47]. To investigate if astrocytes influence caspase-3 activity, we analyzed cell lysate of neurons treated with astrocyte-conditioned media on western blot (Figure 7A). Treatment of neuronal cultures with Aβ1-42 10 μM for 48 h significantly increased the amount of cleaved caspase-3 in cell lysate, when compared to control cells. Pretreatment with different concentrations of ARN14494, from 1 μM to 10 μM, reduced the β-amyloid-induced accumulation of cleaved caspase-3 (Figure 7B). These results suggest that secreted factors from astrocytes may intensify caspase-3 activation in response to β-amyloid.

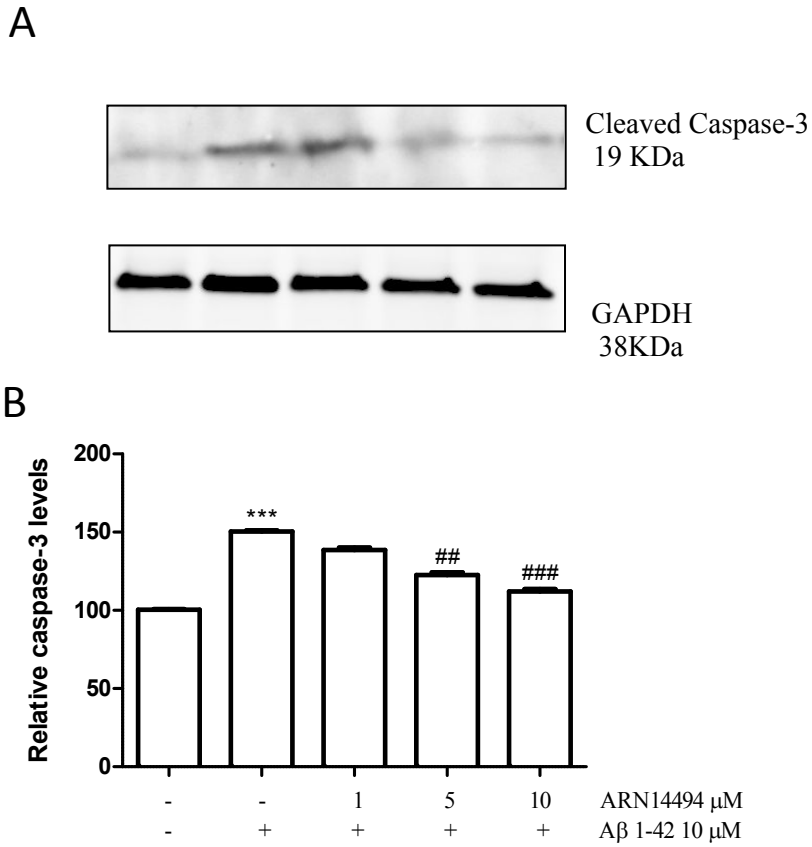

Figure 7. Astrocyte-conditioned medium induced an increase in caspase-3 activity. Western blot (A) of cell lysate from rat primary cortical neurons treated with astrocyte-conditioned medium. Neurons were exposed for 24 h to Aβ1-42 10 μM with and without pretreatment with ARN14494 10 μM. (B) Bar chart showing the amount of cleaved caspase-3 following standardization to GAPDH in each sample. The data presented as mean ± SEM of three individual experiments. ***$p < 0.001$ vs. control, ##$p< 0.01$, ###$p < 0.001$ vs Aβ1-42.

Based on our finding, ARN14494 is a promising selective inhibitor of the serine palmitoyltransferase in an in vitro model of Alzheimer's disease. We demonstrated that ARN14494 decreases SPT activity in a dose-dependent manner in two neuronal cell lines: mouse neuroblastoma Neuro-2a and human astrocytoma CCF-STTG1 cells. We investigated how the downregulation of SPT is accompanied by a decrease of long-chain ceramides (C18:0, C24:0) and dihydroceramides. We used cultured astrocytes and neurons to show that astrocyte have an important role in neurodegeneration. Several studies have demonstrated that soluble factor secreted from astrocytes have an important role in Aβ-induced neurotoxicity. ARN14494 inhibits oligomeric Aβ-induced

overproduction of pro-inflammatory molecules including NO, TNF-α, IL1β, TGF1β, and pro-inflammatory enzymes INOS and COX-2 in cultures of primary astrocytes. It also reduced Aβ neurotoxicity and caspase-3 activation treated with astrocyte-conditioned medium in cultures of cortical neurons. Based on these promising results, we are now planning in vivo studies on ARN14494 to further determine its anti-inflammatory and neuroprotective effects.

METHODS

Chemistry. Chemical synthesis of ARN14494 is provided in the Supporting Information.

Analytical stability is provided in the Supporting Information.

Cell cultures: *Hek293, N2a and CCF-STTG1 cells.* The Hek293 cell line was purchased from ATCC and grown in DMEM medium (Gibco), supplemented with 0.1% penicillin-streptomycin (EuroClone; MI,Italy). The N2a cell line was purchased from ATCC and grown in DMEM medium (Gibco), supplemented with 0.1% penicillin-streptomycin (EuroClone; MI,Italy), 2mM L-glutamine (EuroClone; MI, Italy), and 10% heat-inactivated foetal bovine serum (EuroClone; MI, Italy). The CCF-STTG1 cell line was purchased from Sigma-Aldrich and cultured in RPMI-1640 medium (EuroClone; MI, Italy), supplemented with 0.1% penicillin-streptomycin (EuroClone; MI, Italy), 2mM L-glutamine (EuroClone; MI, Italy), and 10% heat-inactivated foetal bovine serum (EuroClone; MI, Italy). Cells were maintained at 37 °C in a 5% CO_2 humidified atmosphere.

Animals. Female C57BL/6J mice were purchased from Charles River Laboratories (Lecco, Italy). After arrival in our facilities, animals were housed in a temperature-controlled and humidity-controlled room under a 12 h light /dark cycle (lights on at 7 a.m.) with water and food ad libitum. At least 24 h before the experiment, animals were brought to the experimental room and kept in a ventilated storage cabinet (Tecniplast S.p.A.; VA, Italy). Acoustic and olfactory stimuli were kept to a minimum.

Ethics Statement. Experiments were carried out in accordance with Italian regulations on the protection of animals used for experimental purpose (D.M. 116192) and in accordance with European

Economic Community regulations (O.J. of E.C L358/1 12/181986). The protocol was approved by the Italian Ministry of Health.

Primary mouse cortical astrocytes. Mouse primary astrocyte cultures were prepared as previously described [48] with slight modifications. Briefly, on postnatal day 1-3 (P1-3) wild-type C57BL/6J mouse brain cortices were harvested in ice-cold Hank's Balanced Salt Solution (GIBCO Life Technologies; MB, Italy). The midbrain, meninges, and blood vessels were removed by dissection. Tissue were digested in 0.25% Trypsin containing 0.1% EDTA (GIBCO Life Technologies; MB, Italy) at 37 °C for 30 min. Cells were dispersed by gentle trituration, and seeded in Dulbecco's modified Eagle's Medium DMEM (EuroClone; MI, Italy), with 10% fetal bovine serum (FBS; Euroclone; MI, Italy), 1% antibiotic solution (100 U/ml penicillin-100 µg/ml streptomycin), and 2mM L-glutamine (EuroClone; MI, Italy) in 56 cm^2 dishes at $1.5x10^6$ /dish. Cells were grown in the 37 °C incubator with 5% CO_2. After 15 days in vitro, the microglia and oligodendrocyte progenitors were depleted by shaking, and the remaining astrocyte-enriched cultures were harvested from the dishes with trypsin. These cells were cultured for further experiments.

Primary mouse cortical neurons. Primary neuronal cultures were prepared from C57BL/6J mice on embryonic day 16 according to the method described by[49] with some modifications. The neocortices of 16-day mice embryos were collected and subjected to the procedure for isolating the neuronal cells. The cells were seeded in poly-D lysine hydrobromide (Sigma-Aldrich; MI, Italy) coated plate and cultured at 37 °C in a 5% CO_2 humidified atmosphere in neurobasal medium (GIBCO Life Technologies; MB, Italy) supplemented with 2mM L-glutamine, penicillin (100U/ml), streptomycin (100U/ml), (EuroClone; MI, Italy), and 2% B27 (GIBCO Life Technologies; MB, Italy. Neurons were maintained in culture for 5 days in vitro.

Astrocyte-conditioned media (ACM). For preparation of ACM, confluent cultures of astrocytes in 10 cm dishes were washed three times in PBS and fed with 10 ml of neurobasal medium. Astrocytes were treated with drugs for the indicated time. ACM was harvested after 48 h of conditioning and

filtered through a 0.2 μm syringe filter. Cortical neurons were cultured for 48 h and then processed for apoptosis studies.

Microsomal membrane preparation. Cells were scraped off from plates with cold PBS 1X pH 7.4 and collected by centrifugation (500g, 10 minutes, 4°C); cells pellets were re-suspended in buffer (50mM Hepes-NaOH pH8, 1mM EDTA), disrupted by sonication (2X for 20 seconds at 50% power and 50% pulsation) and centrifuged at 2500g for 2 minutes at 4°C. the resultant supernatants collected (total cell lysates) were then centrifuged at 100000g for 30 minutes at 4°C and membranes pellets were re-suspended in buffer (50mM HEPES-NaOH pH8, 1mM EDTA).

Serine palmitoyltransferase Assay. The reactions were performed in triplicate containing 100 μg of microsomal preparation. Assay mix was prepared to achieve the final concentration of 500μM L-serine, 40μM Pyridoxal 5'-phosphate, 100μM Palmitoyl-CoA, and 500nM L-[3H(G)]-Serine (PerkinElmer, NET248250UC, 1mCi/mL, specific activity 15-40 Ci/mmol). The reactions were stopped with the addition, in the following sequence, of 500 μl of 4:1 (MeOH/KOH):CHCl3, 500 μl of CHCl3, 500 μl of alkaline water, and 100 μl of NH4OH 2N. Radioactivity was measured by liquid scintillation counting (Microbeta2 Lumijet, Perkin Elmer Inc.).

Ceramide measurement. Astrocytes were treated with relative compounds for 24 h. Cells were washed twice with ice-cold phosphate-buffer saline, and lipids were extracted with the chloroform/methanol method. The organic phases were collected, dried under nitrogen, and dissolved in methanol/chloroform (3:1, vol/vol) for LC/MS analyses. Ceramides and dihydroceramides were analyzed by LC-MS/MS, using a Waters Acquity UPLC coupled with a Waters Xevo TQMS and interfaced with ESI. Metabolites were separated on a Waters Acquity BEH C18 1.7μm column (2.1 x 50 mm) at 60 °C. A step gradient of 0.1% formic acid in acetonitrile/water (20:80 v/v) as solvent A and 0.1% formic acid in acetonitrile/isopropyl alcohol (20:80 v/v) as solvent B was applied at a flow rate of 0.4 mL/min. Detection was in the positive ionization mode. Capillary voltage was 3.0 kV and cone voltage was 25 V. The source temperature and desolvation temperatures were set at 120 °C and 600 °C, respectively. Desolvation gas and cone gas (N2) flow were 800 and 50 l/h, respectively.

Ceramides were identified based on their LC retention times and MSn fragmentation patterns. Multiple-reaction-monitoring (MRM) mode was used to quantify C14:0 ceramide (m/z 510.0 > 492.0 > 264.0), C16:0 ceramide (m/z 538.0 > 520.0 > 264.0), C18:0 ceramide (m/z 566.0 > 548.0 > 264.0), C20:0 ceramide (m/z 594.0 > 576.0 > 264.0), C22:0 ceramide (m/z 622.2 > 604.27 > 264.3), C24:0 ceramide (C24:0 m/z 650.0 > 632.0 > 264.0), and C24:1 ceramide (C24:1 m/z 648.0 > 630.0 > 264.0). Detection and analysis were controlled by Waters MassLynx software version 4.1. Dihydroceramides (dHCer) were identified based on their LC retention times and MSn fragmentation patterns. Multiple-reaction-monitoring (MRM) mode was used to quantify dHCer 16:0 (m/z 540.5 > 522.5 > 284.5), dHCer 18:0 (m/z 568.5 > 550.5 > 284.5), dHCer 24:0 (m/z 652.5 > 634.5 > 284.5), and dHCer 24:1 (m/z 650.5 > 632.5 > 284.5). The total protein levels were measured by the BCA method. The total ceramides and dihydroceramides levels were normalized to the protein level, and then normalized to the control.[50]

Cell toxicity assay. The CellTiter-Glo® Luminescent Cell Viability Assay (Promega, MI, Italy) was used to determine the number of viable cells in culture. ARN14494 was freshly prepared in dimethylsulphoxide (DMSO), and Amyloid β-Protein 1-42 (Bachem; RM, Italy) was prepared in water. Cells ($2X10^3$) were seeded in 96-well plate in the appropriate culture medium. The next day, astrocytes were pre-treated for 1 h with ARN14494 before treatment with Amyloid β-Protein 1-42 for an additional 24 h. Subsequently, cortical neurons were cultured with ACM for 24 h and processed for cell viability.

Quantitative reverse transcription-polymerase chain reaction. Astrocytes were treated with relative compounds for 3, 6, 12 and 24 h, and their RNA was isolated using the Pure link RNA Mini Kit (Ambion). Real-time PCR procedures were carried out as described previously with some modification[51]. Total RNA was quantified using ND-2000 nanodrop spectrophotometer. Following determination of RNA concentration, 1 μg of total RNA was used for first-strand cDNA synthesis using the SuperScript ViloTM (Invitrogen). cDNA was amplified using quantitative real-time PCR with Assays on Demand premixed TaqMan primer/probe set for mouse TNF-α, IL1β, iNOS, COX2,

TFGβ1 (Applied Biosystem; Foster City, CA), and analyzed using an Applied Biosystems ViiATM7 Real Time PCR System with relative quantification method normalized against HPRT (Applied Biosystem).

Enzyme-linked immunosorbent assay (ELISA). Astrocytes were treated with compounds for the indicated time as previously described. Endogenous mouse TNF- α and IL1β, secreted into the culture media following proinflammatory stimulation, were measured by sandwich enzyme-linked immunosorbent assay (ELISA) kit (R&D Systems, Minneapolis, MN, USA). Optical densities were measured by Tecan microplate reader set to 450 nm wavelength. Each sample was assayed in triplicate, and 3 independent reactions were performed. All readings were normalized to the total cell protein content, and then the data were normalized to the control.

Western Blot. Protein concentrations of the astrocyte lysates were measured using the Pierce BCA protein assay kit (Thermo Scientific, Rockford,IL). Equal amounts (30μg) of protein were separated on 4-15% Mini –Protean® TGXTM Gel (Bio-Rad) and transferred to nitrocellulose membrane. Membranes were then blocked with 5% milk in 0.05% Tween 20-Tris buffered saline for 1 h and incubated overnight at 4 °C with primary antibodies, iNOS (Abcam, Cambridge, MA, USA), COX2 (Abcam, Cambridge, MA, USA), and GAPDH (Millipore, Temecula, CA, USA). After washing in TBST, blots were incubated in (HRP)-conjugated goat anti-mouse (for iNOS 1:5000; for GAPDH 1:5000; 1h at RT) or goat anti-rabbit (for COX2 1:5000; 1h at RT) secondary antibodies. The same procedure was performed for protein concentrations of the neuron lysates. Membrane was incubated with primary antibody cleaved caspase-3 1:1000 (Cell Signaling) in 1% milk, 0.05% Tween 20-Tris buffered saline overnight at 4 °C. After washing in TBST, blot was incubated in (HRP)-conjugated goat anti-rabbit 1:5000 1h at RT. Finally, blots were developed using enhanced chemiluminescence (ECL) LiteAblot® Extend (EuroClone), and digitally imaged using a Fujifilm LAS4000 System. ImageJ software was used to quantify the signal intensity of the protein bands.

Nitrite assay. NO synthesis in astrocytes was measured by a microplate assay method. Total NO metabolite concentration was determined using the Griess assay (Sigma Aldrich). The nitrate

reductase solution 10 µl and enzyme co-factors solution 10 µl were added to the sample. The plate was incubated for 2h at RT. Griess reagent A 50 µl and Griess reagent B 50 µl were added to the plate and incubated for 10 min at 25 °C. The nitrite concentration was then determined by measuring the absorbance at 540 nm.

Hoechst 33342 staining. Following 5 days in vitro, neurons were treated with ACM at 37 °C for 24 h. The cells were washed twice with phosphate-buffered saline (PBS) and stained with Hoechst 33342 staining solution (10 µg/ml). After 15 min of incubation in the dark, the cells were washed 3 times with cold PBS and then examined with the fluorescence microscope.

Statistical analysis. Data are presented as mean ± standard error of mean (SEM). Statistical analysis was performed using 1-way ANOVA followed by Newman-Keuls post-test where appropriate. P levels <0.05 were considered statistically significant. Statistical analysis was performed using Graph Pad Prism version 5.00 (Graph Pad Software, San Diego, USA).

ASSOCIATE CONTENT

Supporting Information

Supporting informations includes: Supporting Figure S1, Figure S2, and Synthesis of ARN14494. This material is available free of charge via the Internet at http://pubs.acs.org.

AUTHOR INFORMATION

Corresponding Author

Andrea Cavalli, PhD

Professor & Research Director

Computational & Chemical Biology

Via Morego 30, 16163 Genova Italy

+39 01071781530

andrea.cavalli@iit.it

ORCID

Teresa De Vita: 0000-0001-7565-6344

Andrea Cavalli: 0000-0002-6370-1176

Author Contributors

Participated in research design: De Vita T., Cavalli A.

Conducted experiments: DeVita T., Albani C.

Contributed new chemical tools: Migliore M.

Performed data analysis: De Vita T. Albani C., Realini N., Basit A., Ottonello G.

Wrote the manuscript: De Vita T.

Contributed to the writing or reading of the manuscript: Cavalli A.

Notes

The authors declare that they have no conflicts of interest with the contents of this article. This work was financially supported by Istituto Italiano di Tecnologia.

ACKNOWLEDGEMENTS

We thank Prof. Piomelli for useful discussion in the initial phases of the project.

ABBREVIATIONS

AD, Alzheimer's disease; CNS, Central Nervous System; SPT, serine palmitoyltransferase; APP, amyloid precursor protein; NO, nitric oxide; IL-1β, interleukin-1β; TNF-α, tumor necrosis factor-α; TGF-β, transforming growth factor β; SPTLC1, serine palmitoyltransferase long chain 1; SPTLC2, serine palmitoyltransferase long chain 2; iNOS, inducible nitric oxide synthase; COX2, cyclooxygenase-2; BACE1, Beta-secretase 1; DMEM, Dulbecco's modified Eagle's Medium; FBS,

fetal bovine serum; HBSS, Hank's Balanced Salt Solution; DMSO, dimethylsulphoxide; ACM Astrocyte-conditioned media.

REFERENCES

1. Huang, Y., and Mucke, L. (2012) Alzheimer mechanisms and therapeutic strategies, *Alzheimer mechanisms and therapeutic strategies 148*, 1204-1222.

2. LaFerla, F. M., and Oddo, S. (2005) Alzheimer's disease: Abeta, tau and synaptic dysfunction, *Trends in molecular medicine 11*, 170-176.

3. Yankner, B. A. (1996) Mechanisms of neuronal degeneration in Alzheimer's disease, *Neuron 16*, 921-932.

4. Hardy, J., and Selkoe, D. J. (2002) The amyloid hypothesis of Alzheimer's disease: progress and problems on the road to therapeutics, *Science 297*, 353-356.

5. Iqbal, K., and Grundke-Iqbal, I. (2008) Alzheimer neurofibrillary degeneration: significance, etiopathogenesis, therapeutics and prevention, *Journal of cellular and molecular medicine 12*, 38-55.

6. Lum, H., and Roebuck, K. A. (2001) Oxidant stress and endothelial cell dysfunction, *American journal of physiology. Cell physiology 280*, C719-741.

7. Smith, M. A., Rottkamp, C. A., Nunomura, A., Raina, A. K., and Perry, G. (2000) Oxidative stress in Alzheimer's disease, *Biochim. Biophys. Acta 1502*, 139-144.

8. Puglielli, L., Tanzi, R. E., and Kovacs, D. M. (2003) Alzheimer's disease: the cholesterol connection, *Nat. Neurosci. 6*, 345-351.

9. Bush, A. I. (2003) The metallobiology of Alzheimer's disease, *Trends Neurosci. 26*, 207-214.

10. Gsell, W., Jungkunz, G., and Riederer, P. (2004) Functional neurochemistry of Alzheimer's disease, *Curr. Pharm. Des. 10*, 265-293.

11. Schliebs, R., and Arendt, T. (2006) The significance of the cholinergic system in the brain during aging and in Alzheimer's disease, *Journal of neural transmission (Vienna, Austria : 1996) 113*, 1625-1644.

12. Walton, H. S., and Dodd, P. R. (2007) Glutamate-glutamine cycling in Alzheimer's disease, *Neurochem. Int. 50*, 1052-1066.

13. Zarros, A., Kalopita, K. S., and Tsakiris, S. T. (2005) Serotoninergic impairment and aggressive behavior in Alzheimer's disease, *Acta Neurobiol Exp (Wars) 65*, 277-286.

14. Carro, E., and Torres-Aleman, I. (2004) The role of insulin and insulin-like growth factor I in the molecular and cellular mechanisms underlying the pathology of Alzheimer's disease, *Eur. J. Pharmacol. 490*, 127-133.

15. Akiyama, H., Barger, S., Barnum, S., Bradt, B., Bauer, J., Cole, G. M., Cooper, N. R., Eikelenboom, P., Emmerling, M., Fiebich, B. L., Finch, C. E., Frautschy, S., Griffin, W. S., Hampel, H., Hull, M., Landreth, G., Lue, L., Mrak, R., Mackenzie, I. R., McGeer, P. L., O'Banion, M. K., Pachter, J., Pasinetti, G., Plata-Salaman, C., Rogers, J., Rydel, R., Shen, Y., Streit, W., Strohmeyer, R., Tooyoma, I., Van Muiswinkel, F. L., Veerhuis, R., Walker, D., Webster, S., Wegrzyniak, B., Wenk, G., and Wyss-Coray, T. (2000) Inflammation and Alzheimer's disease, *Neurobiol. Aging 21*, 383-421.

16. Lucas, S. M., Rothwell, N. J., and Gibson, R. M. (2006) The role of inflammation in CNS injury and disease, *Br. J. Pharmacol. 147 Suppl 1*, S232-240.

17. Akiyama, H., Arai, T., Kondo, H., Tanno, E., Haga, C., and Ikeda, K. (2000) Cell mediators of inflammation in the Alzheimer disease brain, *Alzheimer Dis. Assoc. Disord. 14 Suppl 1*, S47-53.

18. Kitazawa, M., Yamasaki, T. R., and LaFerla, F. M. (2004) Microglia as a potential bridge between the amyloid beta-peptide and tau, *Ann. N. Y. Acad. Sci. 1035*, 85-103.

19. Tansey, M. G., McCoy, M. K., and Frank-Cannon, T. C. (2007) Neuroinflammatory mechanisms in Parkinson's disease: potential environmental triggers, pathways, and targets for early therapeutic intervention, *Exp. Neurol. 208*, 1-25.

20. Block, M. L., Zecca, L., and Hong, J. S. (2007) Microglia-mediated neurotoxicity: uncovering the molecular mechanisms, *Nature reviews. Neuroscience 8*, 57-69.

21. Eikelenboom, P., Zhan, S. S., van Gool, W. A., and Allsop, D. (1994) Inflammatory mechanisms in Alzheimer's disease, *Trends Pharmacol. Sci. 15*, 447-450.

22. Ho, G. J., Drego, R., Hakimian, E., and Masliah, E. (2005) Mechanisms of cell signaling and inflammation in Alzheimer's disease, *Current drug targets. Inflammation and allergy 4*, 247-256.

23. Morgan, D. (2005) Mechanisms of A beta plaque clearance following passive A beta immunization, *Neuro-degenerative diseases 2*, 261-266.

24. Pan, X. D., Zhu, Y. G., Lin, N., Zhang, J., Ye, Q. Y., Huang, H. P., and Chen, X. C. (2011) Microglial phagocytosis induced by fibrillar beta-amyloid is attenuated by oligomeric beta-amyloid: implications for Alzheimer's disease, *Molecular neurodegeneration 6*, 45.

25. Cutler, R. G., Kelly, J., Storie, K., Pedersen, W. A., Tammara, A., Hatanpaa, K., Troncoso, J. C., and Mattson, M. P. (2004) Involvement of oxidative stress-induced abnormalities in ceramide and cholesterol metabolism in brain aging and Alzheimer's disease, *Proc. Natl. Acad. Sci. U. S. A. 101*, 2070-2075.

26. Han, X., D, M. H., McKeel, D. W., Jr., Kelley, J., and Morris, J. C. (2002) Substantial sulfatide deficiency and ceramide elevation in very early Alzheimer's disease: potential role in disease pathogenesis, *J. Neurochem. 82*, 809-818.

27. Satoi, H., Tomimoto, H., Ohtani, R., Kitano, T., Kondo, T., Watanabe, M., Oka, N., Akiguchi, I., Furuya, S., Hirabayashi, Y., and Okazaki, T. (2005) Astroglial expression of ceramide in Alzheimer's disease brains: a role during neuronal apoptosis, *Neuroscience 130*, 657-666.

28. Geekiyanage, H., and Chan, C. (2011) MicroRNA-137/181c regulates serine palmitoyltransferase and in turn amyloid beta, novel targets in sporadic Alzheimer's disease, *J. Neurosci. 31*, 14820-14830.

29. Holland, W. L., Brozinick, J. T., Wang, L. P., Hawkins, E. D., Sargent, K. M., Liu, Y., Narra, K., Hoehn, K. L., Knotts, T. A., Siesky, A., Nelson, D. H., Karathanasis, S. K., Fontenot, G. K., Birnbaum, M. J., and Summers, S. A. (2007) Inhibition of ceramide synthesis ameliorates glucocorticoid-, saturated-fat-, and obesity-induced insulin resistance, *Cell metabolism 5*, 167-179.

30. Patil, S., Melrose, J., and Chan, C. (2007) Involvement of astroglial ceramide in palmitic acid-induced Alzheimer-like changes in primary neurons, *Eur. J. Neurosci. 26*, 2131-2141.

31. Patil, C. S., Singh, V. P., Satyanarayan, P. S., Jain, N. K., Singh, A., and Kulkarni, S. K. (2003) Protective effect of flavonoids against aging- and lipopolysaccharide-induced cognitive impairment in mice, *Pharmacology 69*, 59-67.

32. Weiss, B., and Stoffel, W. (1997) Human and murine serine-palmitoyl-CoA transferase--cloning, expression and characterization of the key enzyme in sphingolipid synthesis, *Eur. J. Biochem. 249*, 239-247.

33. Hannun, Y. A., and Obeid, L. M. (2008) Principles of bioactive lipid signalling: lessons from sphingolipids, *Nature reviews. Molecular cell biology 9*, 139-150.

34. Merrill, A. H., Jr., Nixon, D. W., and Williams, R. D. (1985) Activities of serine palmitoyltransferase (3-ketosphinganine synthase) in microsomes from different rat tissues, *J. Lipid Res. 26*, 617-622.

35. Han, G., Gupta, S. D., Gable, K., Niranjanakumari, S., Moitra, P., Eichler, F., Brown, R. H., Jr., Harmon, J. M., and Dunn, T. M. (2009) Identification of small subunits of mammalian serine palmitoyltransferase that confer distinct acyl-CoA substrate specificities, *Proc. Natl. Acad. Sci. U. S. A. 106*, 8186-8191.

36. Petrache, I., Natarajan, V., Zhen, L., Medler, T. R., Richter, A. T., Cho, C., Hubbard, W. C., Berdyshev, E. V., and Tuder, R. M. (2005) Ceramide upregulation causes pulmonary cell apoptosis and emphysema-like disease in mice, *Nat. Med. 11*, 491-498.

37. Park, T. S., Rosebury, W., Kindt, E. K., Kowala, M. C., and Panek, R. L. (2008) Serine palmitoyltransferase inhibitor myriocin induces the regression of atherosclerotic plaques in hyperlipidemic ApoE-deficient mice, *Pharmacol. Res. 58*, 45-51.

38. Miklosz, A., Lukaszuk, B., Baranowski, M., Gorski, J., and Chabowski, A. (2013) Effects of inhibition of serine palmitoyltransferase (SPT) and sphingosine kinase 1 (SphK1) on palmitate induced insulin resistance in L6 myotubes, *PloS one 8*, e85547.

39. Liu, L., Martin, R., and Chan, C. (2013) Palmitate-activated astrocytes via serine palmitoyltransferase increase BACE1 in primary neurons by sphingomyelinases, *Neurobiol. Aging 34*, 540-550.

40. Geekiyanage, H., Upadhye, A., and Chan, C. (2013) Inhibition of serine palmitoyltransferase reduces Abeta and tau hyperphosphorylation in a murine model: a safe therapeutic strategy for Alzheimer's disease, *Neurobiol. Aging 34*, 2037-2051.

41. da Cunha, A., and Vitkovic, L. (1992) Transforming growth factor-beta 1 (TGF-beta 1) expression and regulation in rat cortical astrocytes, *J. Neuroimmunol. 36*, 157-169.

42. Lefebvre, P. P., Martin, D., Staecker, H., Weber, T., Moonen, G., and Van de Water, T. R. (1992) TGF beta 1 expression is initiated in adult auditory neurons by sectioning of the auditory nerve, *Neuroreport 3*, 295-298.

43. Flanders, K. C., Lippa, C. F., Smith, T. W., Pollen, D. A., and Sporn, M. B. (1995) Altered expression of transforming growth factor-beta in Alzheimer's disease, *Neurology 45*, 1561-1569.

44. Stewart, V. C., and Heales, S. J. (2003) Nitric oxide-induced mitochondrial dysfunction: implications for neurodegeneration, *Free Radic. Biol. Med. 34*, 287-303.

45. Zhu, D. Y., Deng, Q., Yao, H. H., Wang, D. C., Deng, Y., and Liu, G. Q. (2002) Inducible nitric oxide synthase expression in the ischemic core and penumbra after transient focal cerebral ischemia in mice, *Life Sci. 71*, 1985-1996.

46. Garwood, C. J., Pooler, A. M., Atherton, J., Hanger, D. P., and Noble, W. (2011) Astrocytes are important mediators of Abeta-induced neurotoxicity and tau phosphorylation in primary culture, *Cell death & disease 2*, e167.

47. Cribbs, D. H., Poon, W. W., Rissman, R. A., and Blurton-Jones, M. (2004) Caspase-mediated degeneration in Alzheimer's disease, *Am. J. Pathol. 165*, 353-355.

48. McCarthy, K. D., and de Vellis, J. (1980) Preparation of separate astroglial and oligodendroglial cell cultures from rat cerebral tissue, *J. Cell Biol. 85*, 890-902.

49. Frandsen, A., and Schousboe, A. (1990) Development of excitatory amino acid induced cytotoxicity in cultured neurons, *Int. J. Dev. Neurosci. 8*, 209-216.

50. Busik, J. V., Reid, G. E., and Lydic, T. A. (2009) Global analysis of retina lipids by complementary precursor ion and neutral loss mode tandem mass spectrometry, *Methods Mol. Biol. 579*, 33-70.

51. Heid, C. A., Stevens, J., Livak, K. J., and Williams, P. M. (1996) Real time quantitative PCR, *Genome Res. 6*, 986-994.

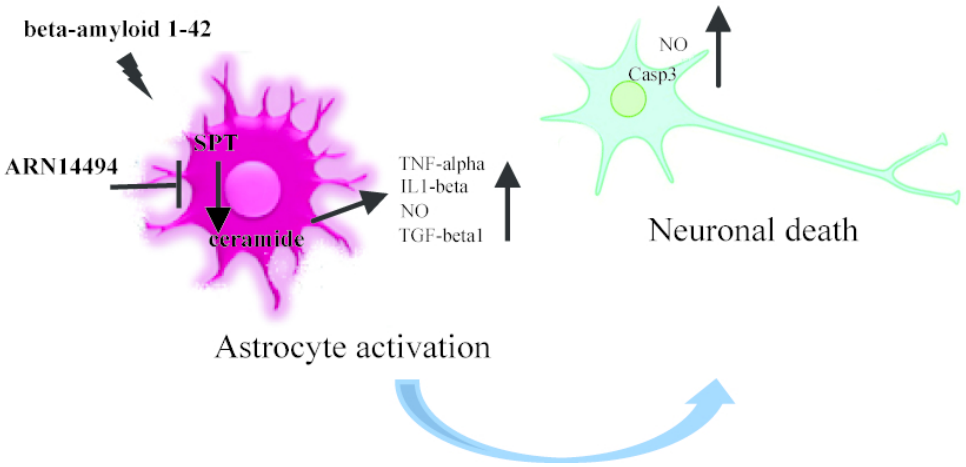
beta-amyloid 1-42
ARN14494
SPT
ceramide
TNF-alpha
IL1-beta
NO
TGF-beta1
NO
Casp3
Neuronal death
Astrocyte activation

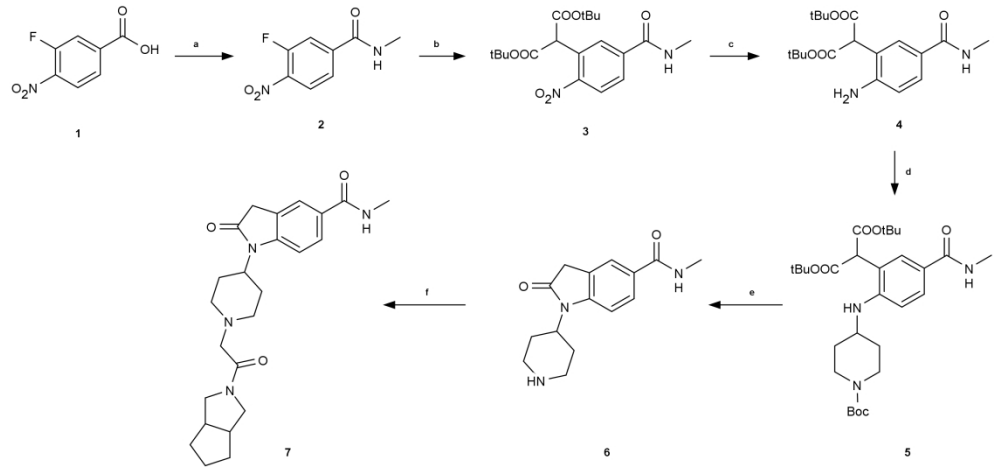

Table 1. Synthesis of compound ARN14494. a) oxalyl chloride; MeHN2·HCl, TEA, H2O, 0 °C, 94%; b) ditButylmalonate, NaH, DFM, 64%; c) Pd/C, HCOONH4, MeOH, 100%; d) N-BOC-piperidone, AcOH, NaBH(OAc)3, DCE, 60%; e) TosOH, Tol/H2O, 100 °C, 87%; f) R-COCH2Cl, K2CO3, ACN/H2O, 68%.

383x190mm (232 x 232 DPI)

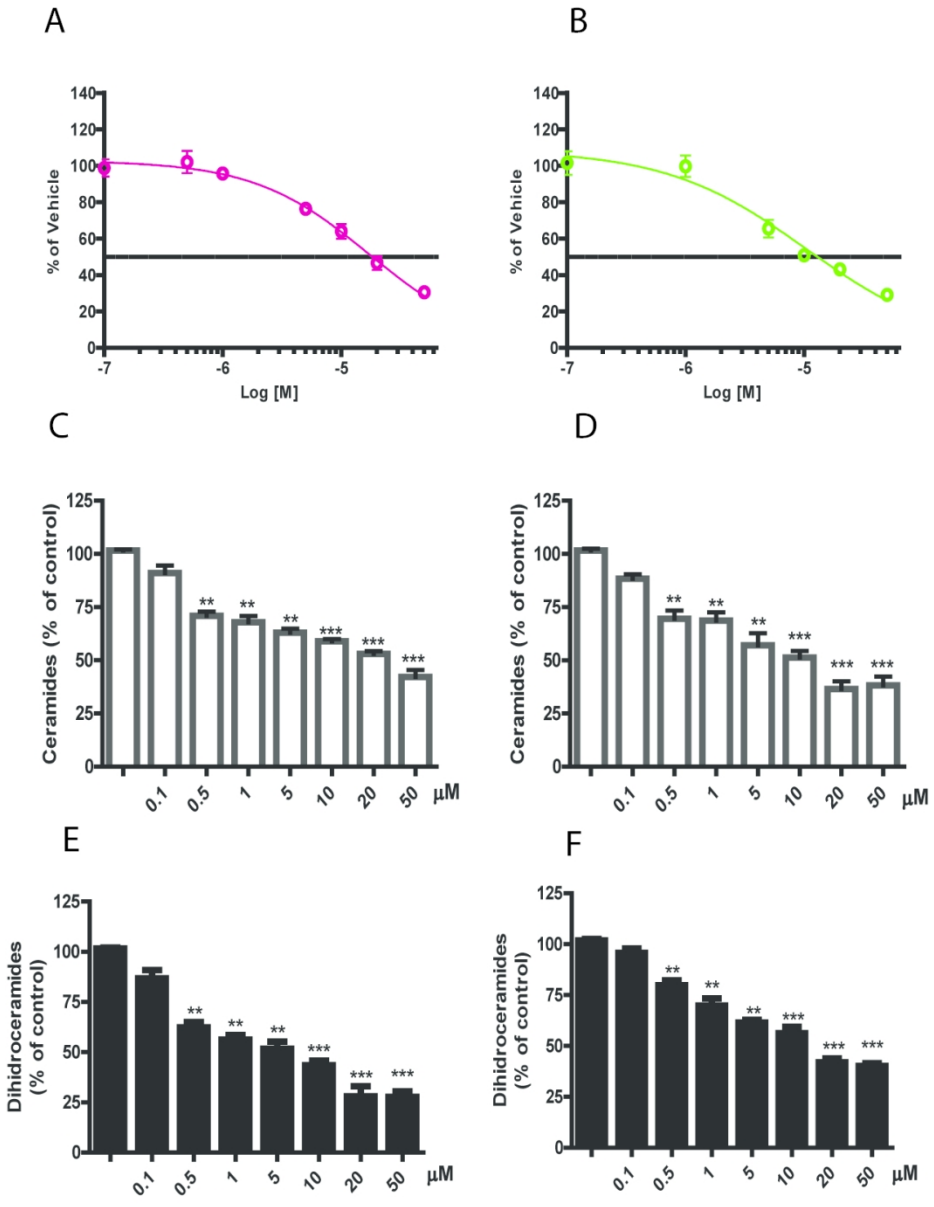

ARN14494 is a potent SPT inhibitor, and it decreases ceramide and dihidroceramide levels in mouse Neuro-2a and human CCFSTTG1 cells. Effects of ARN14494 (n=3) on SPT activity in mouse N2a (Fig. 1A) and human CCFSTTG1 (Fig. 1B) cells. Effects of ARN14494 on ceramide and dihidroceramide levels in Neuro-2a (Fig. 1 C-E) and CCFSTTG1 (Fig. 1 D-F) cells. Data represent mean ± SEM of three independent experiments performed in triplicate. **p<0.01, ***p<0.001 vs CTRL. One-way ANOVA followed by Newman-Keuls test.

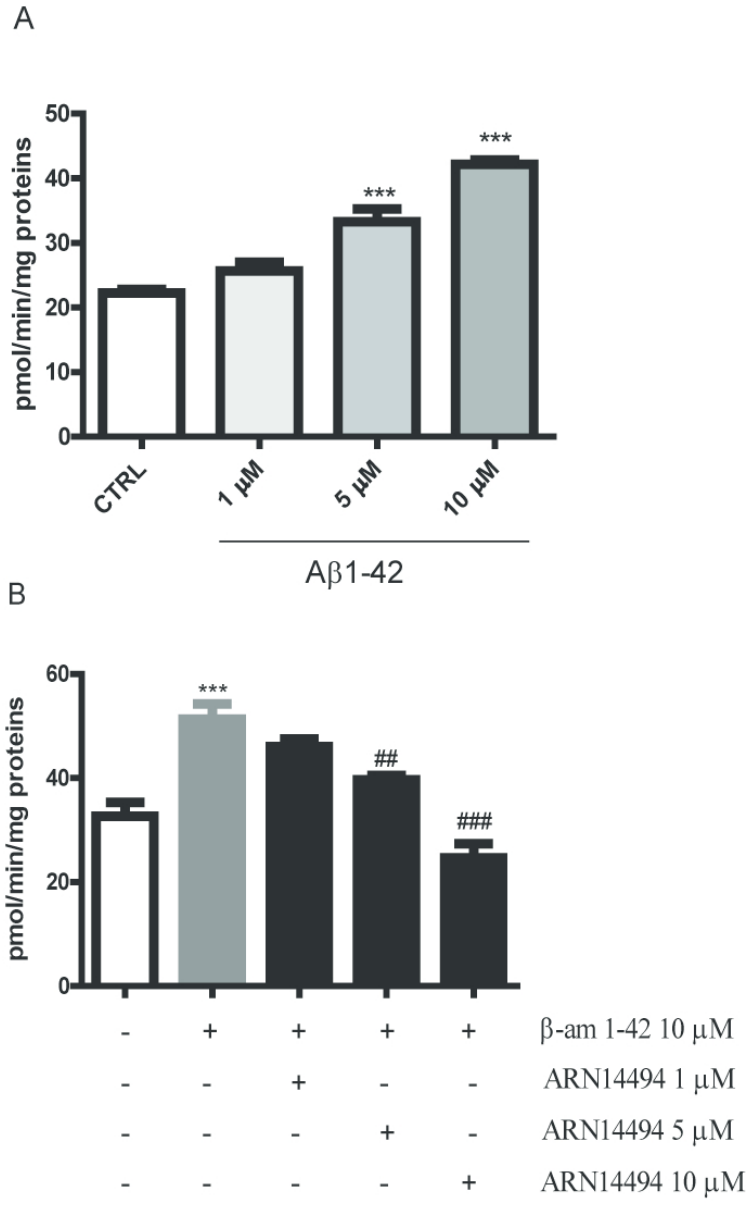

Figure 2. ARN14494 inhibits SPT activity in mouse primary astrocytes. Effect of an increase dose of Aβ1-42 on SPT activity in mouse primary astrocytes (Fig. 2A). Effect of an increase of ARN14494 on SPT activity in mouse primary astrocytes (Fig 2B). Data represent mean ± SEM of three independent experiments. ***p<0.001 vs CTRL, ##p<0.01, ###p<0.001 vs Aβ1-42. One-way ANOVA followed by Newman-Keuls test.

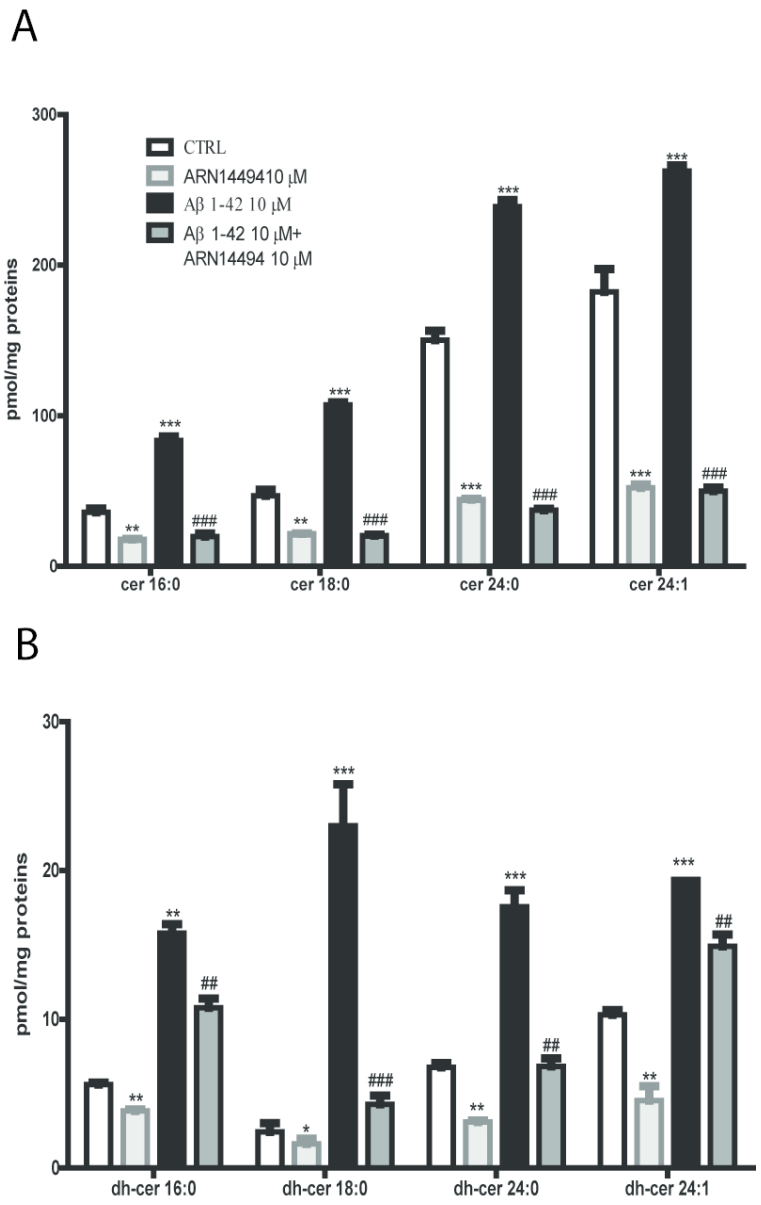

ARN14494 decreases ceramide and dihidroceramide levels in primary cortical astrocytes treated with Aβ1-42. Effects of ARN14494 at 24h of incubation on different ceramide (A) and dihidroceramide (B) levels on mouse primary astrocytes treated with Aβ1-42 10μM. Data represent mean ± SEM of three independent experiments performed in triplicate. *p<0.05, **p<0.01, ***p<0.001 vs ctrl, ##p<0.01, ###p<0.001 vs Aβ1-42 10μM. Two-way ANOVA followed by Bonferroni's test.

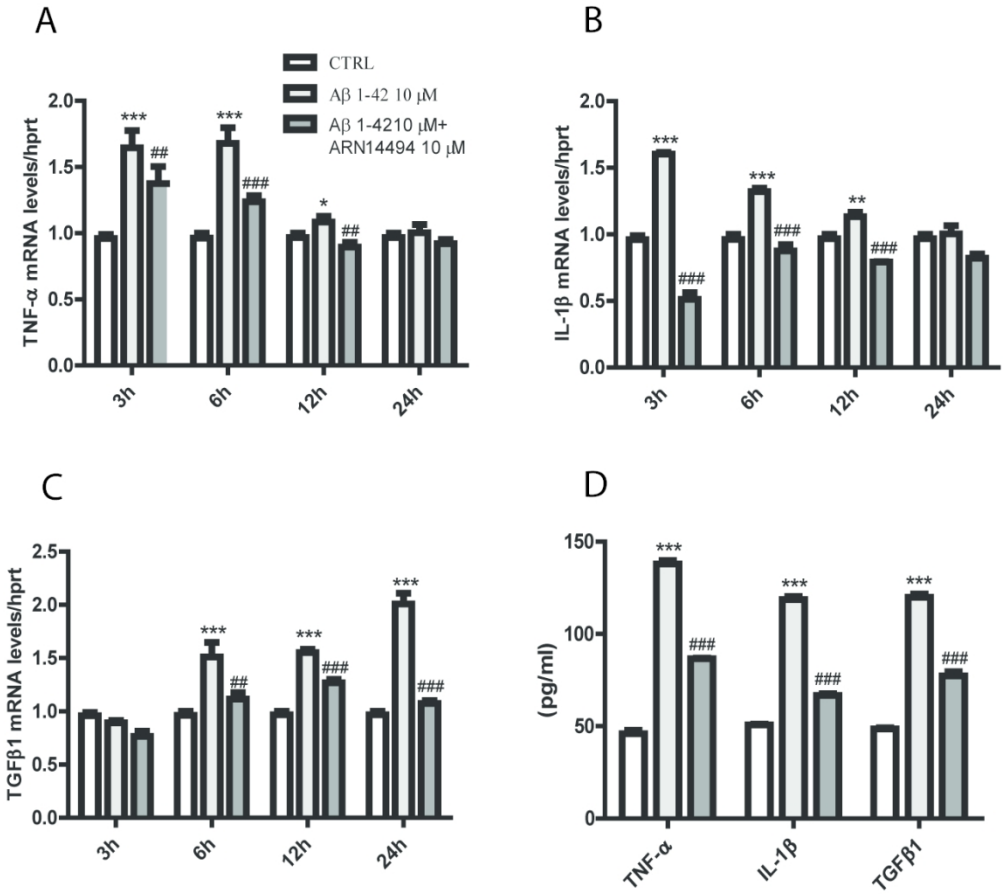

Effect of ARN14494 on Aβ1-42-induced expression of TNF-α, IL1 β, and TGF-1β mRNA and production of TNF-α, IL1 β, and TGF-1β. Primary astrocytes were pretreated with 10 μM of ARN14494 for 24 h. Intact cells were treated with 10 μM of Aβ1-42, then TNF-α (A), IL1 β (B), and TGF-1β (C) mRNA expression was measured 3-6-12-24 h later in cell lysates. Protein production was measured 24 h later in cell medium (D). Data represent mean ± SEM of three independent experiments. *p<0.05, **p<0.01, ***p<0.001 vs CTRL, #p<0.05, ##p<0.0, ###p<0.001 vs Aβ1-42. One-way ANOVA followed by Newman-Keuls test.

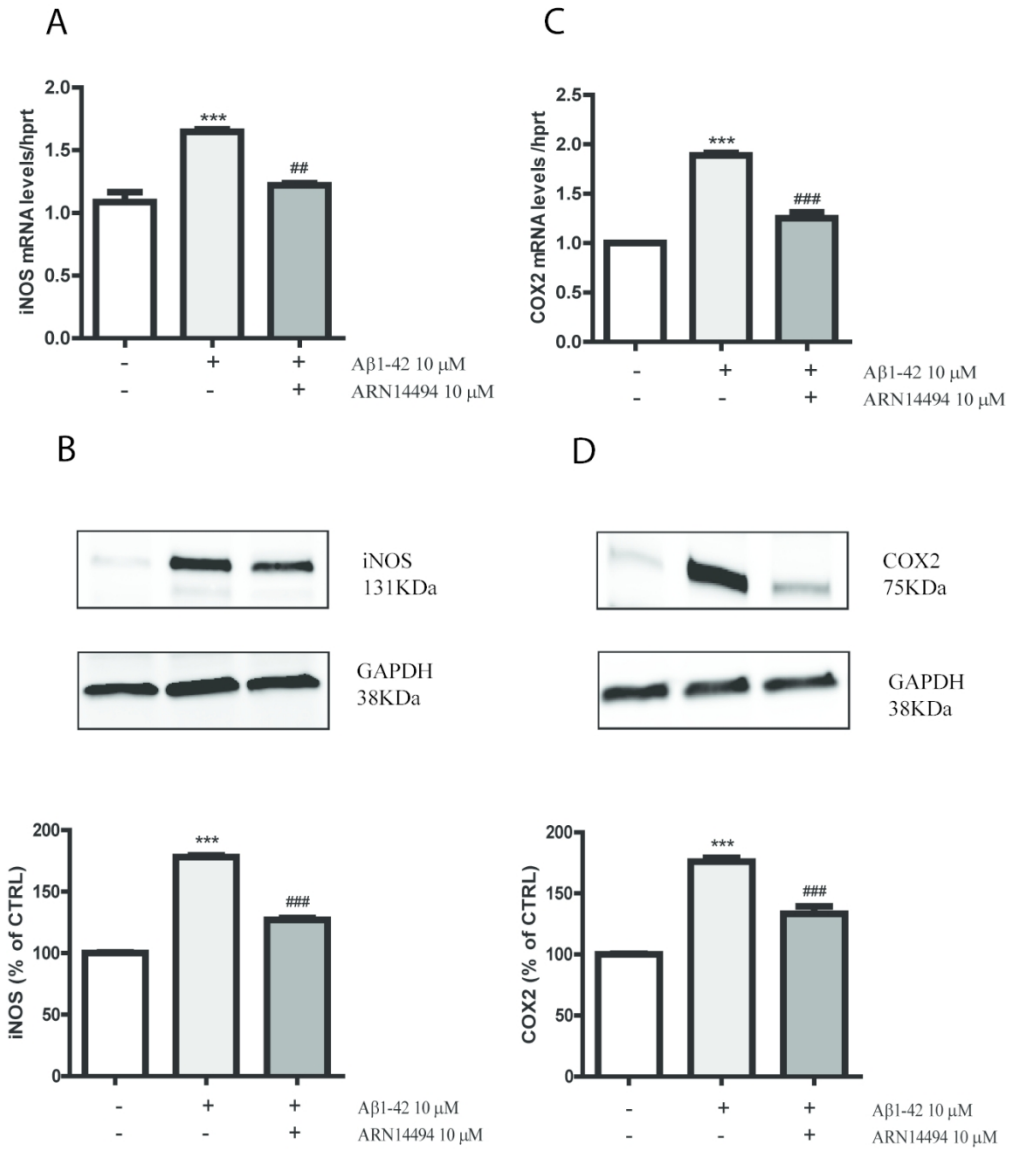

. Effect of ARN14494 on Aβ1-42-induced iNOS, COX2 mRNA expression and iNOS, COX2 protein expression. Primary astrocytes were pretreated with 10 μM of ARN14494 for 24 h. Intact cells were treated with 10 μM of Aβ1-42, then iNOS (A) and COX2 (C) mRNA expression was measured 6 h later in cell lysates. The protein expression of iNOS (B) and COX2 (D) was measured by Western blot 24 h later, and data normalized by GAPDH. Data represent mean ± SEM of three independent experiments. **p<0.01, ***p<0.001 vs CTRL, ##p<0.01 vs Aβ1-42. One-way ANOVA followed by Newman-Keuls test

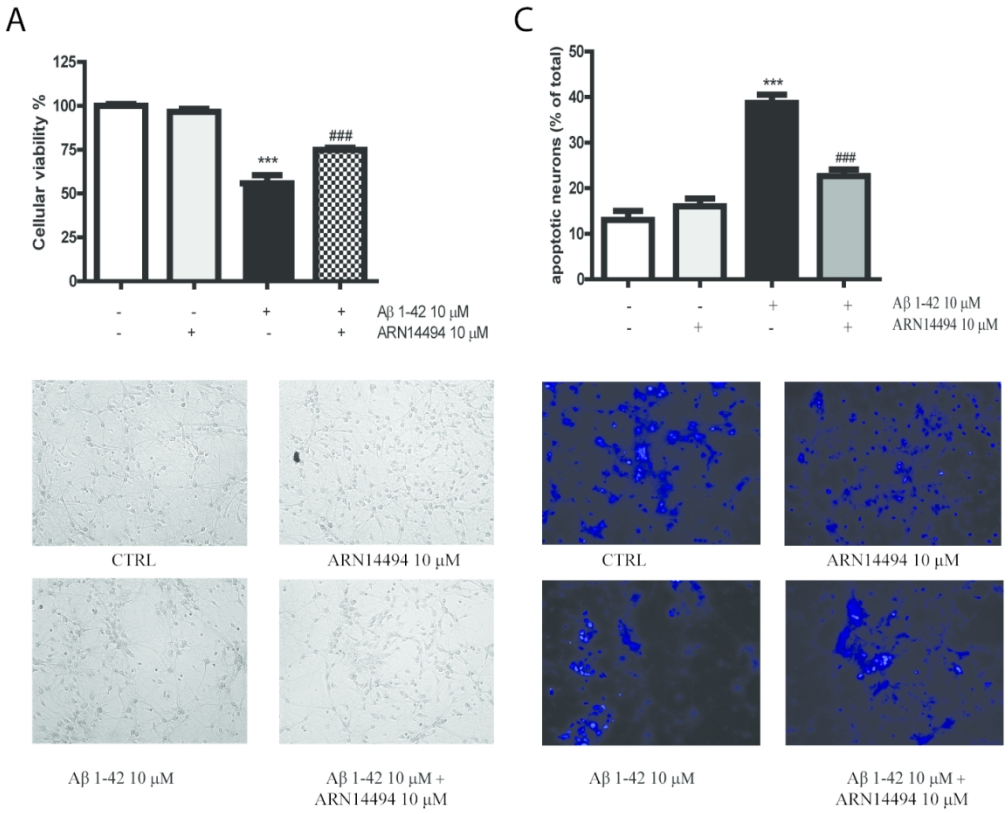

Factors secreted from astrocytes mediate β-amyloid-induced neurotoxicity. Primary cortical neurons were treated for 48 h with conditioned medium from mouse primary astrocytes treated with 10 μM Aβ1-42 and/or 10 μM ARN14494. Values are ATP release from neurons into medium, expressed as percentage of CTRL (6A). ARN14494 inhibits Aβ1-42-induced neuron apoptosis. (B) The morphological features of apoptosis were monitored by fluorescence microscopy after staining with Hoechst 33342. Neurons that exhibited reduced nuclear size, chromatin condensation, intense fluorescence, and nuclear fragmentation were considered apoptotic. Pretreatment with ARN14494 10 μM for 24 h decreased the number of apoptotic neurons during Aβ1-42 injury. (C) Quantitative analysis of apoptotic neurons. Data represent mean ± SEM of three independent experiments. ***p<0.001 vs CTRL, ###p<0.001 vs Aβ1-42. One-way ANOVA followed by Newman-Keuls test.

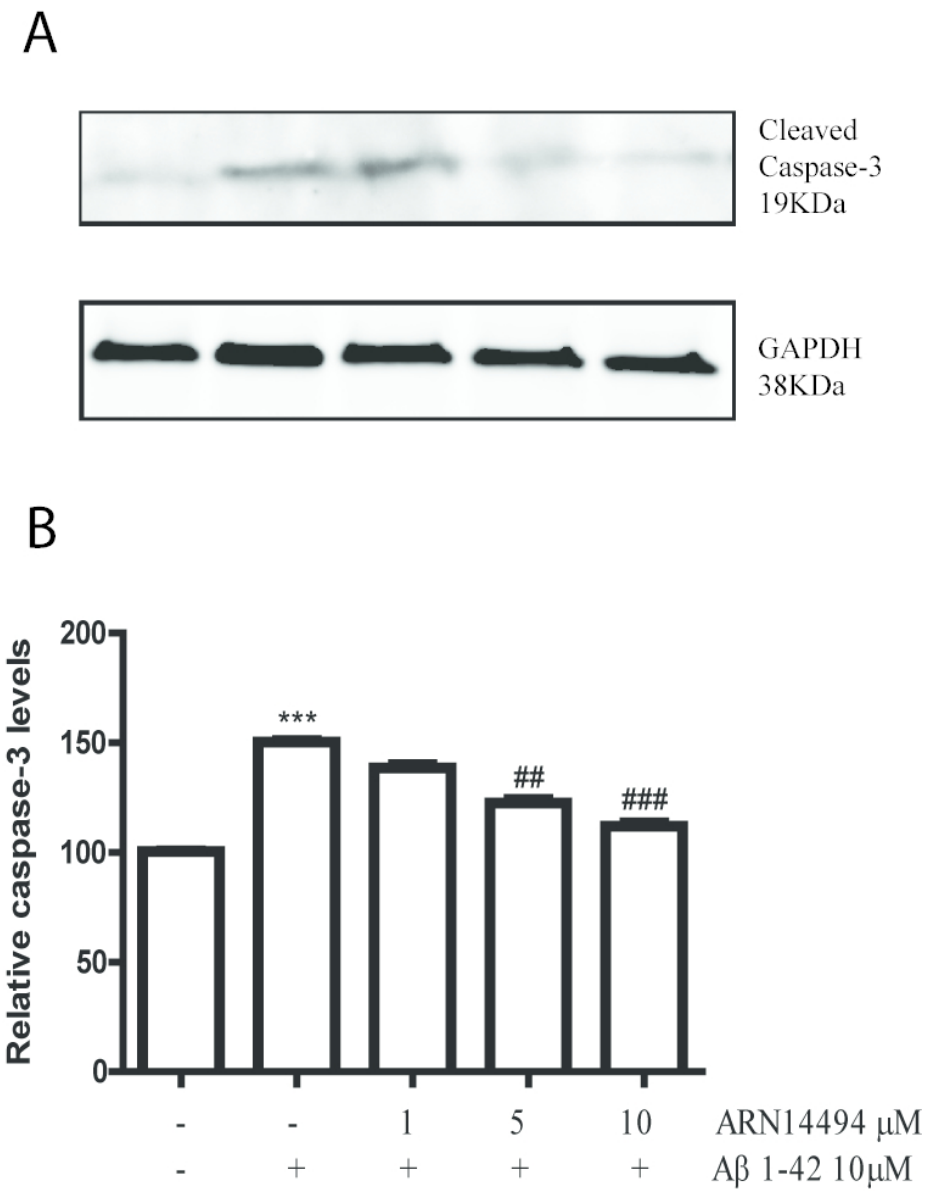

Astrocyte-conditioned medium induced an increase in caspase-3 activity. Western blot (A) of cell lysate from rat primary cortical neurons treated with astrocyte-conditioned medium. Neurons were exposed for 24 h to Aβ1-42 10 μM with and without pretreatment with ARN14494 10 μM. (B) Bar chart showing the amount of cleaved caspase-3 following standardization to GAPDH in each sample. The data presented as mean ± SEM of three individual experiments. ***p < 0.001 vs. control, ##p< 0.01, ###p < 0.001 vs Aβ1-42.

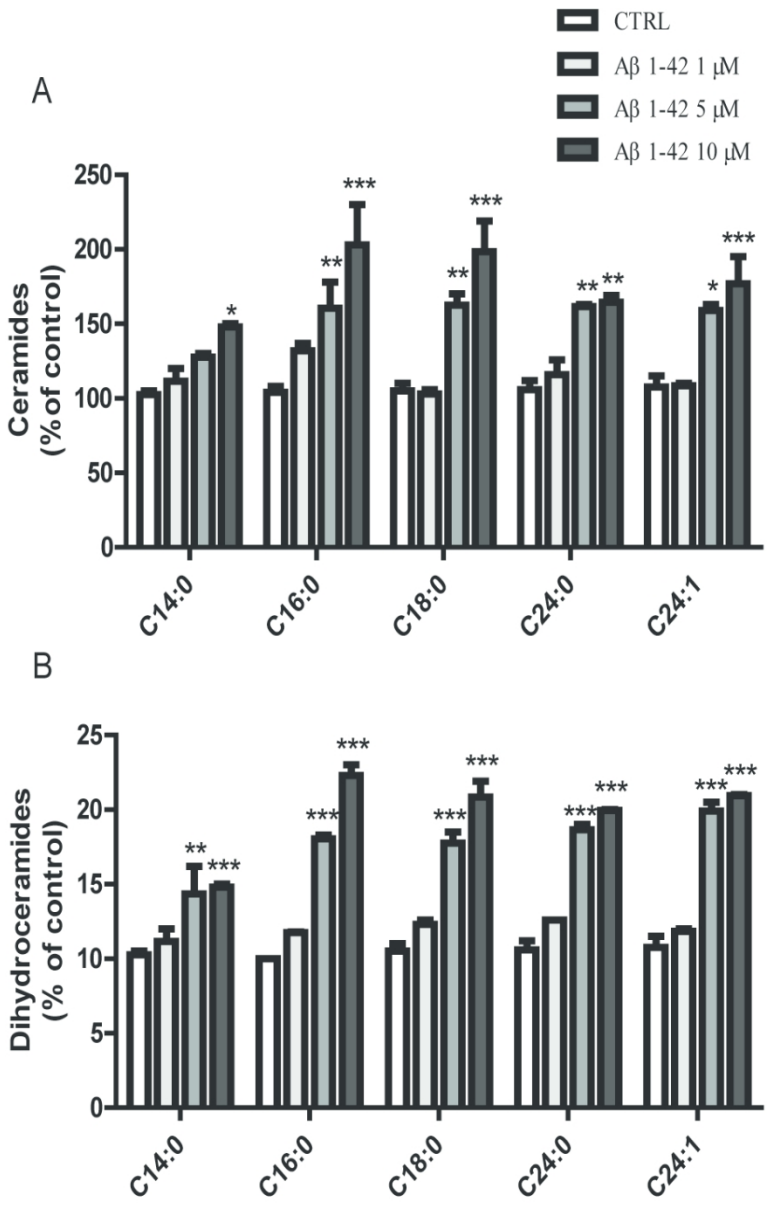

Figure S1. Aβ1-42 increases ceramide and dihydroceramide levels in primary cortical astrocytes. Effect of Aβ1-42 after 24h of incubation at different concentrations (1-5-10 μM) in mouse primary astrocytes on different ceramide (A) and dihydroceramide (B) levels. Data represent mean ± SEM of three independent experiments performed in triplicate. *p<0.05, **p<0.01, ***p<0.001 vs ctrl. Two-way ANOVA followed by Bonferroni's test.

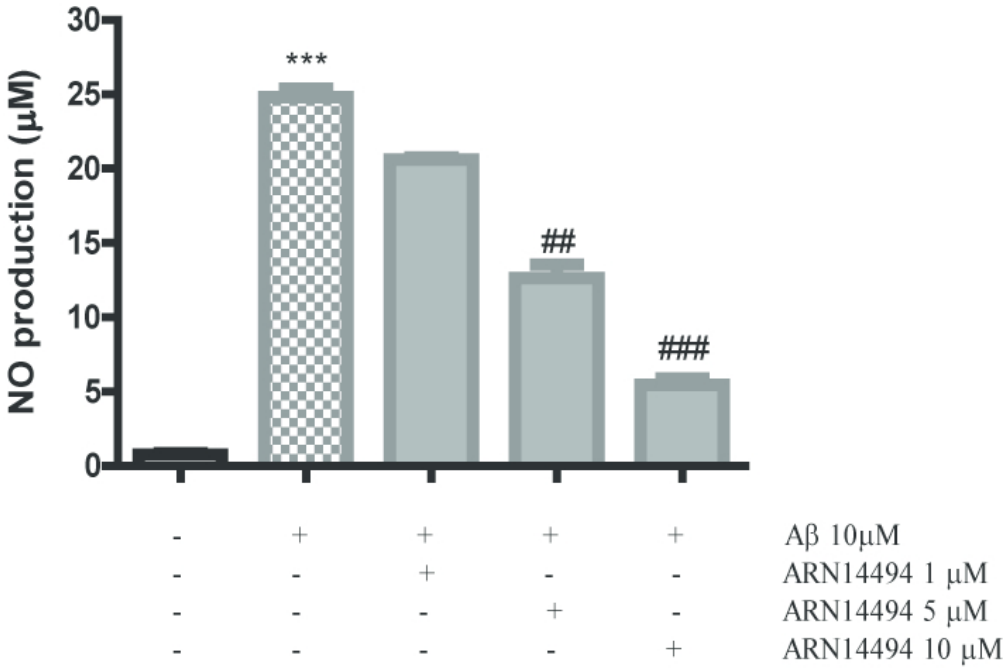

ARN14494 inhibits NO production in Aβ1-42-treated astrocytes. Primary cortical astrocytes were treated with Aβ1-42 10 μM for 24 h and then with an increased dose of ARN14494 (1-5-10 μM). Nitrite content was measured using the Griess reaction. Data represent mean ± SEM of three independent experiments. ***p<0.001 vs CTRL, ##p<0.01, ###p<0.001 vs Aβ1-42. One-way ANOVA followed by Newman-Keuls test.